

# MODELING THE OCEANIC GENERAL CIRCULATION

*James C. McWilliams*

Department of Atmospheric Sciences and Institute of Geophysics and Planetary Physics, University of California, Los Angeles, California 90095-1565

**KEY WORDS:** ocean modeling, climate, ocean circulation, parameterization, computational fluid dynamics

## ABSTRACT

This article reviews the history, formulation, and solution behavior of relatively comprehensive numerical models for the oceanic general circulation under equilibrium surface wind stress and buoyancy flux forcing. The issues of model formulation are both the customary and alternative dynamical approximations of the fundamental fluid dynamics, the parameterization of essential processes that occur on spatial and temporal scales smaller than can be resolved in model calculations, the boundary and initial conditions, the domain geometry, and the numerical algorithms. The solution features discussed here are the wind- and buoyancy-driven lateral gyres in enclosed basins, the mostly longitudinal currents near the equator and around Antarctica, the overturning circulations, the chemical property distributions, and both forced and spontaneous variations about the time-mean circulation, occurring with both meso- and large-scale flow structures.

---

## 1. INTRODUCTION

The practice of oceanic numerical modeling has grown explosively in recent years. Reasons for this include the widespread realization that model solutions can, either now or in the near future, skillfully mimic observed oceanic features; an understanding of the limitations of the alternative and more traditional

scientific methodologies of making measurements in the oceans and of developing analytic theories for its highly nonlinear dynamics; an appreciation of the importance of the oceans in the compelling problems of anthropogenic changes in climate and the environment; and an exploitation of the increases in computing power that make meaningful oceanic calculations much more feasible.

The oceanic general circulation is defined as the currents on horizontal space and time scales larger than the mesoscale (of order 100 km and three months); the associated pressure, density, temperature, and salinity fields; plus all other elements involved in establishing the dynamical balances for these fields. The latter includes the forcing fields, the domain geometry, and the transport contributions by motions on smaller scales. In some conceptions the general circulation also includes the biogeochemical processes associated with other material property fields.

The scope of this review is the formulation and quasi-equilibrium solution behavior of oceanic general circulation models (OGCMs) that span at least an individual basin, if not the global domain, and that include forcing by both surface wind stress and buoyancy (heat and water) flux. Consideration is also given to those material properties, called *tracers*, whose biogeochemical reactions are not too determinative and complex [see Sarmiento (1992) for more reactive chemical properties]. Thus, excluded are most of the applications of OGCMs that can make them so useful: dynamical coupling with the atmosphere, sea ice, and land runoff that in reality jointly determine the oceanic boundary fluxes (e.g. El Niño); interpretation of the paleoclimate record; climate prediction for both natural variability and anthropogenic changes; assimilation of observations to provide dynamically consistent syntheses; pollution dispersal; and fisheries and other biospheric management. Also excluded are more regional and idealized modeling, except where they elucidate OGCM solution behavior.

OGCMs are a relatively recent development. Their conception owes much to the prior example of atmospheric GCMs developed primarily for weather prediction. The roster of pioneers might begin with Sarkisyan (1962), who performed a very short integration for the North Atlantic basin. Quasi-equilibrium solutions in an idealized basin were calculated by Bryan & Cox (1967, 1968) and, including tracers, by Holland (1971). The first global solutions were obtained by Cox (1975) and Takano (1975). Broadly summarized, the history of OGCM solutions is firstly to model only the largest scales of motion with an excessively coarse numerical grid and a concomitant excessively linear and diffusive dynamics representing, or parameterizing, the effects of unresolved, or sub-grid-scale (SGS), motions. Subsequently, more ambitious problems are posed that refine the grid, reduce the SGS diffusivities and thereby increase the

nonlinearity of the dynamics, and examine both forced fluctuations and intrinsic variability arising from instabilities of large-scale currents; the most prominent mode of variability is mesoscale eddies. An increasingly broad range of scales of motion is thereby incorporated into the OGCM solutions, thus decreasing the scope of the requisite SGS parameterizations. Nevertheless, it is inconceivable that a numerical model could incorporate all excited degrees of freedom [of  $\mathcal{O}(10^{40})$  if 1 mm and 1 s are taken as the minimum scales], so SGS parameterizations will always be essential elements of an OGCM. Presently, the frontiers of OGCM calculations lie either in duration among fluctuations of decadal or longer periods or in spatial resolution within the range of mesoscale motions.

Among many previous review articles about OGCMs are those by Pond & Bryan (1976), Holland et al (1983), and Haidvogel & Bryan (1992).

## 2. MODEL FORMULATION

Since the earliest use of OGCMs there has been a remarkable constancy in the physical and algorithmic formulation of the model, even though, as discussed below in Sections 2.5–6, there are defensible alternatives. Bryan (1969) established the paradigm, and many scientists since then have created varietal forms.

### 2.1 *Dynamical Approximations*

The fundamental fluid dynamics of oceanic circulation is the Navier-Stokes equations on the rotating Earth for a compressible liquid, seawater, which is comprised of water plus a suite of dissolved salts that occur in nearly constant ratio but variable amount (the salinity  $S$ ), with an empirically determined equation of state. The equations in an OGCM are based on several substantial simplifications to this more fundamental set (see Veronis 1973 for an extended discussion).

Mass conservation is approximated as the volume conservation of an incompressible fluid, and variations of density  $\rho$  are neglected everywhere in the momentum balances except in the gravitational force (sometimes called the Boussinesq approximation). The basis for these approximations is  $\delta\rho \ll \rho_0$  (where  $\rho_0$  is the mean density), which is true in the ocean to  $\mathcal{O}(1)\%$ . The principal consequence is the exclusion of acoustic waves from the model, consistent with the small Mach number of the general circulation.

The momentum equation in the vertical direction, locally parallel to the gravitational force, is approximated as hydrostatic balance. This is accurate for thin flow patterns with small aspect ratio,  $H/L \ll 1$  (where  $H$  and  $L$  are characteristic vertical and horizontal length scales). These patterns are the only ones that can be resolved with the anisotropic grids used in OGCMs, whose horizontal grid size is typically larger than the ocean depth  $H_*$ . It is an

even more accurate approximation for motions with small Rossby and Froude numbers,  $Ro = U/fL \ll 1$  and  $Fr = U/NH \ll 1$  (where  $U$  is a characteristic horizontal velocity,  $f$  a Coriolis frequency for the Earth's rotation, and  $N$  a buoyancy frequency due to stable density stratification). Both of these parameters are commonly small for large-scale currents, except near the equator where  $f \rightarrow 0$  or in regions of convection (i.e. strong vertical mixing caused by unstable stratification) where  $N \rightarrow 0$ . The principal consequences of the hydrostatic approximation are an inaccuracy in calculating vertically propagating gravity waves and an inability to calculate the strong vertical accelerations that occur in convection. Insofar as these are significant elements of the general circulation, then their effects must be represented in SGS parameterizations (see Section 2.2).

Two other approximations are also based upon the thinness of oceanic currents. One is the neglect of the Coriolis force of the component of the Earth's rotation vector perpendicular to the local vertical direction. Only near the equator and on relatively small spatial scales is this approximation potentially harmful for the general circulation (see e.g. Colin de Verdiere & Schopp 1994). The other is the neglect of the radial metric terms in spherical coordinates because of the relatively small variation in the radial (i.e. locally vertical) coordinate over the ocean depth, i.e.  $H_*/a \ll 1$ , where  $a$  is the mean radius of the Earth.

Until quite recently the common practice has been to assume the ocean has a rigid lid at the top, across which no fluid volume is transferred, although momentum, heat, and chemical composition are. The basis for this is  $\delta H_* \ll H_*$ , where  $\delta H_*$  is the actual variation in sea level; averaged over surface gravity waves and tides and within a given glaciological era,  $\delta H_* = \mathcal{O}(1)$  m. This assumption excludes surface gravity waves and badly distorts tidal dynamics, both of whose interactions with the general circulation are insignificant except perhaps indirectly through their roles in SGS transport near the surface or bottom. It also distorts the propagation of long barotropic (i.e. vertically uniform) Rossby waves with horizontal scales larger than the external deformation radius,  $R_e = \sqrt{gH}/f = \mathcal{O}(2000)$  km, but these modes are sufficiently fast,  $\mathcal{O}(100)$  m s<sup>-1</sup>, that the distortion does little harm for their role in the much slower general circulation. In the case of salinity flux across the upper surface, there is a further approximation because it is actually water, not salt, that is exchanged by evaporation and precipitation. The basis for an approximate equivalence between salt and water fluxes is a linearization about the mean salinity (i.e.  $\delta S/S_0 \ll 1$ ) to define a virtual salinity flux. Huang (1993) argues against this approximation in favor of the *natural boundary condition* of water exchange.

The result of all these approximations is the boundary-value problem for the *primitive equations* in a thin spherical shell:

$$\begin{aligned} \frac{Du}{Dt} - \left( f + \frac{u \tan \phi}{a} \right) v &= -\frac{1}{a \cos \phi} \frac{\partial P}{\partial \lambda} + SGS \\ \frac{Dv}{Dt} + \left( f + \frac{u \tan \phi}{a} \right) u &= -\frac{1}{a} \frac{\partial P}{\partial \phi} + SGS \\ \frac{\partial P}{\partial z} + \frac{g\rho}{\rho_0} &= 0 \\ \frac{1}{a \cos \phi} \left( \frac{\partial u}{\partial \lambda} + \frac{\partial v \cos \phi}{\partial \phi} \right) + \frac{\partial w}{\partial z} &= 0 \\ \frac{D(T, S)}{Dt} &= SGS \\ \rho &= \rho(T, S, P). \end{aligned} \tag{1}$$

Here  $(\lambda, \phi, z)$  are longitude, latitude, and height;  $(u, v, w)$  are the associated velocities;  $P$  is the pressure divided by  $\rho_0$ ;  $T$  is the potential temperature (i.e. invariant under adiabatic compression);  $g$  is the gravitational acceleration;  $f = 2\Omega \sin \phi$ , where  $\Omega$  is the Earth's rotation rate; and  $D/Dt$  is the substantial time derivative,

$$\frac{D}{Dt} = \frac{\partial}{\partial t} + \frac{u}{a \cos \phi} \frac{\partial}{\partial \lambda} + \frac{v}{a} \frac{\partial}{\partial \phi} + w \frac{\partial}{\partial z}. \tag{2}$$

Where  $SGS$  appears in (1) there are important, small-scale, nonconservative processes that provide spatial transports and pathways to the dissipation that actually occurs by molecular kinetic processes on scales of  $\mathcal{O}(1)$  mm. Implicitly these equations are the result of a low-pass filter at the space-time resolution of the numerical model, with  $SGS$  denoting the contributions from the unresolved scales. These equations can be augmented by additional tracer equations similar to those for  $(T, S)$ , adding whichever chemical reactions are required.

## 2.2 Parameterizations

The default form for the  $SGS$  terms in (1) is anisotropic diffusion along the coordinate directions, with a larger diffusivity in the horizontal direction than in the vertical, and larger for horizontal velocity than for tracers, with spatially uniform diffusivities. The physical basis for the anisotropy is the thinness of the ocean and its usually stable stratification, both of which suppress vertical motions relative to horizontal ones. Tracer transport happens only by local movement of matter, whereas momentum transport also happens nonlocally through pressure forces and can thus be greater. Diffusion spreads the influence of the surface forcing, so that an equilibrium state can occur with this default

form. Such a SGS model is, of course, very simple, and it is essential for progress in OGCMs to refine the SGS forms, based both on observations and smaller-scale models of the relevant processes and on assessments of the SGS influences on OGCM solutions.

In the surface planetary boundary layer (PBL), small-scale turbulence is relatively strong because of shear and buoyancy instabilities resulting from the surface fluxes. In the default SGS form, the PBL is implicitly contained within the top grid cell, since there are no elevated diffusivities in the grid interior. An essential extension beyond the default form is to increase the SGS transport where the density stratification is gravitationally unstable (i.e. with a positive vertical gradient in potential density), mimicking the convection that cannot be resolved in (1). This is often done either by *convective adjustment* (a minimal vertical rearrangement of tracers is performed until stable stratification is achieved) or by a substantial enhancement of the vertical diffusivities in the unstable region. Insofar as the instability arises from negative surface buoyancy flux, then the PBL extends from the surface throughout the adjusted or enhanced region. Preferable to this, however, is an explicit boundary layer model for the PBL transport. The most commonly used types in OGCMs have been either bulk mixed-layer models (e.g. Kraus & Turner 1967) or single-point, moment-closure, turbulence models (e.g. Mellor & Yamada 1982). Large et al (1994) review the usage of oceanic boundary layer models and propose a SGS diffusivity-profile model that does not impose such strong constraints on boundary layer profiles as the former and escapes the dubious spatial locality assumption of the latter. As yet, though, no boundary layer model for OGCMs includes the widespread and probably important effects of enhanced mixing by breaking surface gravity waves and wave-driven Langmuir cells.

There is an analogous PBL at the ocean bottom, driven principally by boundary stress without any significant buoyancy flux. A primary effect of the bottom PBL is to provide a drag force on the adjacent flow. Usually in OGCMs this is represented as a boundary stress proportional to  $\mathbf{v}$  or  $\mathbf{v}^2$ , acting only on the deepest grid cell. Obviously, an explicit PBL model, of the types discussed above, could also be used at the bottom. Topography, however, does modify the dynamics (Dietrich et al 1987, 1990). Armi (1978) and Garrett (1991) argue for the possible importance of tracer transport parallel to the boundary by PBL turbulence, but this effect has not yet been examined in an OGCM.

Within the stably stratified oceanic interior, the most energetic SGS motions are the approximately geostrophic (i.e. with a dominant horizontal momentum balance between Coriolis and pressure-gradient forces) mesoscale eddies. They are the primary agents underlying the horizontal diffusion in the default SGS model. The idea of horizontal momentum diffusion is based on the enstrophy

cascade caused by horizontal advection in geostrophic turbulence that transfers vorticity (i.e.  $\hat{\mathbf{z}} \cdot \nabla \times \mathbf{v}$ ) from larger scales to smaller ones (Charney 1971). Horizontal tracer diffusion is more doubtful because gravitational work is required to move matter across surfaces of neutral buoyancy (i.e. isopycnal surfaces), and these surfaces typically are tilted from the horizontal in geostrophic balance with the currents. A parameterization of mesoscale tracer transport by Gent & McWilliams (1990) that is isopycnally oriented and integrally adiabatic (i.e. without interior sources or sinks of any material property that alters its inventory on isopycnal surfaces) has had quite beneficial effects on OGCM tracer distributions and fluxes (Danabasoglu et al 1994, Boening et al 1995a). In addition to tracer diffusion along isopycnals (Redi 1982), the parameterization has an incompressible, eddy-induced transport velocity  $\mathbf{v}^*$  that combines with  $\mathbf{v}$  to advect the tracers (Gent et al 1995) and thereby causes vertical transport of momentum and depletion of potential energy, as in baroclinic instability. Mesoscale eddies also can mix potential vorticity [another conservative material invariant of (1) for a simplified  $\rho(T, S, P)$ ] along isopycnal surfaces (Marshall 1981, McWilliams & Chow 1981, Rhines & Young 1982), and this potentially offers a basis for refining the SGS parameterization of momentum transport. Even in OGCM calculations that partially resolve the mesoscale eddy spectrum, the preceding SGS issues are likely to be significant.

There are various small-scale processes, in addition to convection, that can make the mixing across interior isopycnals be spatially and temporally nonuniform; note that such effects are inherently nonadiabatic, in the sense defined above. They are usually represented as a vertical flux, since this direction is very nearly perpendicular to isopycnal surfaces over most of the ocean, whose typical slopes are  $\mathcal{O}(10^{-4})$ . Most notable among these processes are stratified shear instability, breaking internal waves, and double diffusion caused by the larger molecular diffusivity of  $T$  than of  $S$ ; Large et al (1994) review their SGS parameterization forms. Pacanowski & Philander (1981) show that shear instability, with vertical diffusivity  $\kappa_v$  varying inversely with Richardson number,  $Ri = N^2/(\partial \mathbf{v}/\partial z)^2$ , influences the equatorial undercurrent and thermocline profiles in OGCM solutions. Demonstrations of possibly substantial consequences on the abyssal tracer distributions are presented in Cummins et al (1990) and Cummins (1991), for breaking internal waves with  $\kappa_v$  varying inversely with  $N$ , and in Gargett & Holloway (1992), for double diffusion with unequal  $\kappa_v$  values for  $T$  and  $S$ . The nonlinearity in  $\rho(T, S, P)$  also allows for locally enhanced vertical transport through thermobaric and cabbeling instabilities, and Garwood et al (1994) show that the former can be of significance in the surface PBL in subpolar regions. Although the effects of density nonlinearity are present in principle in OGCM solutions that have enhanced vertical

diffusivity in the presence of convective instability, their significance has yet to be assessed.

### 2.3 *Boundary and Initial Conditions*

The usual boundary conditions for an OGCM with a rigid lid are no normal flow at all land and air boundaries, specified tracer flux (zero on the sides and bottom), specified surface stress, an internally determined bottom stress (see above), and zero horizontal slip velocity on the sides, which also implies an internally determined boundary stress. A plausible generalization of the dynamically uncertain side boundary condition for large-scale  $v$  is to let the tangential stress be proportional to the horizontal slip; variation of the proportionality constant indicates that this condition can exert substantial control over an OGCM wind-driven gyre circulation (i.e. recirculation largely within a horizontal plane) and its associated boundary current separation (McWilliams et al 1990, Haidvogel et al 1992). For subglobal domains with open-water side boundaries, model variables must be specified either empirically or by internally determined outflow or radiation conditions. Obviously, care must be taken that these side conditions do not exert excessive control over the calculated solutions; in practice, wind-driven circulations are more often dynamically closed within individual basins than are the more global buoyancy-driven (i.e. thermohaline) circulations.

The surface stress is due to the drag by the overlying wind, and it is calculated from a wind climatology. Surface tracer flux might also be specified from a climatology. However, the accuracy of any such climatology is highly problematic, especially for water flux, both because the measurements are difficult and because each is the result of many nearly canceling processes (i.e. sensible and latent heat fluxes, solar and infrared radiation, evaporation and precipitation, ice formation and melting, and river runoff). Furthermore, experience shows that the use of specified climatological heat and water fluxes can yield OGCM solutions that diverge significantly from a  $(T, S)$  climatology, reflecting both flux and modeling inaccuracies. Rather than mount a direct attack on this problem, by broadly exploring flux and modeling alternatives, the common practice has instead been to specify the tracer flux indirectly. The simplest procedure for this is to use *restoring conditions*, in which the surface tracer equations are forced by the difference between a climatological value and the model value divided by a restoring time constant of  $\mathcal{O}(\text{days-months})$ . The implied surface fluxes have spatially noisy patterns, again especially so for water flux, although with climatologically plausible large-scale magnitudes. And, of course, the resulting surface tracer values do not differ too greatly from climatology. More sophisticated variants have been developed in which the restoring value and time constant vary spatially and temporally to

bring both the surface tracer and its flux closer to climatology (Haney 1971, Han 1984, Barnier et al 1995), and Tziperman & Bryan (1993) suggest an iterative procedure using the resulting OGCM solutions to further refine the flux estimates. A physical rationalization of the thermal restoring condition is that there should be a local negative feedback with the overlying atmosphere to damp (on the restoring time) an oceanic surface temperature anomaly, although no such local feedback argument can be made for a salinity anomaly that does not influence the overlying atmosphere except indirectly and nonlocally through changes in the circulation. Rahmstorf & Willebrand (1995) and Seager et al (1995) have made proposals for weakening this feedback as the horizontal scale of the  $T$  anomaly increases (implying a more responsive atmosphere, hence a weaker damping of the anomaly through surface heat flux). For some OGCM problems, particularly those concerned with natural variability, alternative *mixed conditions* are employed for tracers, in which  $T$  is either specified or restored and the flux of  $S$  is specified, usually by diagnosing a preliminary solution with fully restoring conditions (e.g. Bryan 1986). Mixed conditions are both somewhat more plausible in relation to the local atmospheric feedbacks and more conducive to natural variability than fully restoring conditions. As discussed in Section 3.4 below, there is abundant evidence that OGCM solution stability and variability are sensitive to the surface tracer conditions, which are both empirically uncertain and physically indeterminate entirely within an ocean model. Perhaps this aspect of model formulation cannot be adequately resolved until there are sufficiently skillful coupled atmosphere-ice-ocean models. It is likely that the oceanic PBL parameterization will play a much more influential role in both OGCM and coupled problems for which sea-surface temperature is not as highly constrained as it is with restoring conditions.

Typical OGCM initial conditions are climatological  $T$  and  $S$  fields and zero motion. From such a state there is geostrophic adjustment to the tracer fields within days and boundary-, Kelvin-, and Rossby-wave adjustments to the wind forcing within years that generate currents that at least grossly resemble those in the equilibrium state. The equilibrium state occurs only after thousands of years in which advection and SGS transport have redistributed the tracers consistent with the OGCM problem as posed [see Sugimotohara & Fukasawa (1988) and Danabasoglu et al (1995) for analyses of spin-up]. Unless approximately correct tracer fields are given as initial conditions, an OGCM solution will differ greatly from its equilibrium state after only a several-year integration. Scientists who wish to avoid the costly computations to reach full equilibrium nevertheless bear the burden of demonstrating that shorter integration times do not excessively bias their solutions. At present it is computationally infeasible to integrate a global OGCM to equilibrium with mesoscale resolution.

## 2.4 Domain Geometry

The shape of ocean basins is determined by bottom topography, including its intersection with the top surface, the coastline. Topography has a profound influence on the direction of currents, especially near the bottom. The reason for this is the approximate material conservation of potential vorticity, whereby a change in the thickness  $h$  between an interior isopycnal surface and the bottom implies a compensating change in the fluid vorticity that acts to turn the fluid trajectory towards a path of constant  $f/h$ . Illustrations of this influence for deep circulation patterns are made in Speer et al (1993).

It is far less certain, however, when and where topography fundamentally controls the existence and strength of the large-scale currents. The latter are largely accelerated by internal pressure gradient forces, which through hydrostatic balance and the equation of state are closely related to  $(T, S)$  distributions. Momentum balance against this acceleration can be provided either internally by large-scale advection and SGS transport or by topographic effects such as *topographic form stress* (i.e. integrated horizontal pressure force on the bottom), boundary-layer drag, and *hydraulic control* (wherein throughflow is limited by a critical Froude number). This competition can be posed conceptually as a comparison of model solutions with simpler, smoother topography and ones with rougher, more complex topography. While the desire for geographical realism favors the latter, assurance of computational accuracy favors the former (i.e. accurate numerical solutions require smoothness near the grid scale). There is no satisfactory resolution of these issues at present. Increasing the grid resolution, by incorporating finer topographic details, at least diminishes the scope of the ambiguity in specifying the degree of topographic smoothness.

Munk & Palmen (1951) argue for the importance of topographic form stress in establishing the depth-integrated transport of the Antarctic Circumpolar Current, and this view is well supported in many subsequent OGCM solutions (e.g. Gill & Bryan 1971, McWilliams et al 1978, Stevens & Ivchenko 1995). In mid-latitude basins with longitudinal boundaries, the baroclinic (i.e. depth varying, with  $\nabla P \times \nabla \rho \neq 0$ ) topographic torque, closely related to the topographic form stress, can also contribute significantly to the gyre transport balance (e.g. Sarkisyan & Ivanov 1971, Hurlburt et al 1995). It is still uncertain how widespread this effect is. Early estimates with diagnostic OGCM solutions exaggerated its magnitude because of errors in the empirically specified abyssal density field; Ezer & Mellor (1994) have made a recent calculation using this approach. Topographic steering of currents along  $f/h$  contours acts to weaken the topographic torque.

Constricting straits can limit throughflow, either by boundary stress or hydraulic control (e.g. Pratt 1990). In OGCM solutions flows through a strait

whose width is too close to the grid scale will have a primarily viscous dynamics, which likely exaggerates the former and precludes the inertially controlled dynamics of the latter. This presents a scientist with the temptation to artificially widen or deepen the channel to compensate for these biases, but such a choice is intrinsically ad hoc. The two most important straits in the global ocean are the Drake Passage and the Indonesian Archipelago, both of which have large throughflows; demonstrations of the extreme consequences of blocking them entirely can be found in Ishikawa et al (1994) and Hirst & Godfrey (1993), respectively, and coarsely resolved OGCM solutions have about the same transport as is observed when these straits are artificially widened (e.g. Danabasoglu & McWilliams 1995). Straits occur in all sizes, of course, and some will remain sub-grid scale at all foreseeable resolutions. Probably the most important of these is the Strait of Gibraltar, whose throughflow of salty Mediterranean seawater has significance in the  $S$  budget of at least the North Atlantic Ocean; Armi & Farmer (1988) argue for its hydraulic control. There are analogous difficulties with flow over sills and ridges whose size is too close to the grid scale; a notorious example is the Icelandic Ridge across which deep seawater from the Greenland Sea flows into the Atlantic (e.g. Roberts et al 1995).

Small-scale topographic roughness also influences large-scale circulation. The most direct possibility is through a turbulent rectification process where mesoscale eddies above mesoscale topography cause a form stress that drives large-scale currents along large-scale contours of  $f/h$  (Bretherton & Karweit 1975, Bretherton & Haidvogel 1976, Salmon et al 1976). Holloway (1992) argues that this is likely to be a significant effect on continental slopes where these eddies can drive cyclonic rim currents (i.e. ones having the same rotational sense around the basin as  $f$ ). Ebby & Holloway (1994a), using a rough parameterization for rectification, and Hurlburt et al (1995), with very fine mesoscale resolution, show examples of this possibility in OGCM solutions. However, the strength and vertical distribution of this effect are still quite uncertain. A less direct effect of topographic roughness is its tendency to make the vertical structure of mesoscale eddies more surface intensified, which in turn influences their transport properties in the general circulation (Rhines 1977, Owens & Bretherton 1978, Boening 1989).

## 2.5 Numerical Methods

The computational algorithms that have been used for OGCMs have mostly been rather simple ones, as presented in Bryan (1969) and by others with minor variations. They are a finite-difference discretization of Equations (1) and (2), using centered, nearest-neighbor differences that are second-order accurate in the grid spacing for regular grids [the usual choice in  $(\lambda, \phi)$ ] and formally first-order for the (usually weakly) nonuniform vertical grids with finer resolution

in the more stably stratified upper ocean. The grids are staggered in their distribution of the dependent variables, using one of several alternative schemes. The spatial difference operators are integrally conservative for tracer content and variance and for kinetic energy. Near the poles extra smoothing is required if the grid spacing becomes very small, as it does on a regular longitude-latitude grid. For a given horizontal grid, a sufficiently large horizontal viscosity is needed for computational stability, either to resolve the viscous boundary layers or to suppress nonlinear instability resulting from the enstrophy cascade. For a given nonuniform vertical grid, a sufficiently large  $\kappa_v$  is needed to dominate the implicit numerical diffusion (Yin & Fung 1991).

The time-stepping is by a mixture of first- and second-order accurate procedures, with time-splitting often used to solve separately for the SGS vertical mixing by an implicit algorithm that is computationally stable for arbitrarily large SGS vertical diffusivity. Thus, the time step size  $\Delta t$  is limited by a CFL (Courant-Friedrich-Lewy) condition for advection, internal gravity wave or barotropic Rossby wave propagation, and SGS lateral transport, with typical non-eddy-resolving grids,  $\Delta t = \mathcal{O}(1)$  hr. To integrate for  $\mathcal{O}(10^3)$  years to approach equilibrium (see Section 2.3 above) thus requires  $\mathcal{O}(10^7)$  time steps or more.

The coarsest spatial grids used in global OGCMs have  $\mathcal{O}(10^5)$  grid points, corresponding to a horizontal spacing of hundreds of kilometers and a vertical spacing of hundreds of meters. To refine the grid resolution to be adequate for mesoscale eddies, with horizontal spacing on the order of the internal deformation radius,  $R_i = NH/f = \mathcal{O}(10)$  km (see 3.4 below), requires an increase in the size of the required grid to  $\mathcal{O}(10^8)$  points. Thus, an OGCM calculation is indeed a very large one. At present it is infeasible to combine full mesoscale resolution with full equilibrium in a single calculation, although it likely will become so within the next decade with better computers. Because this computer power might only be achieved through massive parallelism, pioneering OGCM studies are exploring this type of architecture (e.g. Dukowicz et al 1993, on the Connection Machine, and Bleck et al 1995, on the Cray T3D).

A shortcut for reaching equilibrium can often be taken for non-eddy-resolving OGCMs by *acceleration*, which uses a time-stepping technique in Equation (1) with a larger  $\Delta t$  for  $(T, S)$  than for  $(u, v)$  and a further increase in  $\Delta t$  for the deep tracers (Bryan 1984). The rationale is that the CFL constraint is usually most severe on  $(u, v)$  through the SGS horizontal momentum diffusion and the fastest waves, whereas the constraint for tracers is set by their slower SGS lateral transport and advection, which decreases with depth. Since deep tracers are the slowest solution components to approach their equilibrium values, this acceleration technique can reduce the integration time by a factor of  $\mathcal{O}(100)$ .

If the OGCM approaches a steady solution under steady forcing, then this distortion of the transient dynamics causes only a transient error. Danabasoglu et al (1995) show that, even under periodic seasonal forcing, acceleration leads to a valid equilibrium solution if it is followed by a *synchronous* integration, with uniform  $\Delta t$ , for  $\mathcal{O}(10)$  years to allow the seasonal cycle to equilibrate. No doubt this particular technique has a limited range of validity in model resolution and solution transience, but more robust acceleration methods are well worth seeking because of the high computational cost of OGCMs.

Since far more sophisticated numerical methods than those described above are now well established in other contexts, there is likely to be a spate of numerical developments for OGCMs in the future. Some of the present areas of development are the following: more uniform tilings of the sphere than a regular latitude-longitude grid (e.g. Ebby & Holloway 1994b); higher order spatial and temporal discretizations (e.g. Haidvogel et al 1995); advection operators that are not so prone to creating erroneous extrema (e.g. Leonard 1979); fuller temporal implicitness to escape physically unimportant computational stability limits (e.g. Yavneh & McWilliams 1995); more efficient procedures for solving for a reference-level  $P(\lambda, \phi, t)$  in the vertical integration of the hydrostatic relation, via the barotropic streamfunction, rigid-lid surface pressure (Pinaridi et al 1995), or free-surface elevation (e.g. Dukowicz & Smith 1994); and transformation of the vertical height coordinate to either a potential-density (e.g. Bleck & Chassignet 1994, Lunkeit et al 1995) or a topography-following coordinate (e.g. Ezer & Mellor 1994, Song & Haidvogel 1994). An advantage of a potential-density coordinate may be the relative simplicity and ease in assuring integral conservation properties for the discretized, isopycnally oriented, mesoscale-eddy, SGS operators; a disadvantage may be an uncontrollable sparseness of resolution in weakly stratified regions.

## 2.6 *Alternative Dynamical Formulations*

The general circulation has an approximately geostrophic momentum balance, and one can simplify the primitive equations on this basis. The reasons for simplification are to obtain a model whose dynamical behavior is more comprehensible and whose numerical solution is cheaper, if only so that a more extensive search of the solution space becomes feasible.

The strongest form of this simplification uses the *planetary geostrophic equations*, where all accelerations and nonlinearities are deleted from the horizontal momentum equations in (1). This approximation is useful to the extent that momentum advection and mesoscale transport can be adequately parameterized, especially in the boundary currents. Colin de Verdiere (1988, 1989) and Salmon (1986, 1990) use this model to investigate primarily buoyancy-driven circulations in idealized basins. A variant of this model uses the *large-scale*

*geostrophic equations*, which also retain the horizontal accelerations in (1); it is used as a full OGCM in combination with implicit time-stepping (e.g. Maier-Reimer et al 1993). Both of these model classes are computationally stable with a very much larger  $\Delta t$  than the primitive equations with explicit time-stepping.

A less severe simplification is the *balance equations* that result from a second-order asymptotic expansion of the primitive equations for small Rossby and Froude numbers. The lowest-order expansion model, the quasigeostrophic equations, is not appropriate as an OGCM, principally because of its excessive approximations in (a) a tangent-plane representation of the Earth's spherical geometry in the Coriolis force and (b) the assumed smallness of variations about the horizontal- and time-averaged  $N(z)$ . The balance equations exclude all gravity wave solutions, which is probably an accurate approximation for the general circulation, whose important gravity-wave effects are sub-grid scale. In many tests, the balance equations have been shown to have solutions that match those of suitably initialized primitive equations very closely with only a modest fraction of the computational cost (e.g. Norton et al 1986). In particular, McWilliams et al (1990) use the balance equations to study the wind-driven circulation in an idealized basin. However, it is likely that the cost differentials between simpler models and the primitive equations would significantly diminish if implicit time-stepping were used for the latter.

Alternatively, the dynamical model can be generalized beyond the primitive equations. Here the motivation is to be more physically accurate by not making such strong approximations as those behind (1). For this to be worthwhile, the resulting solutions must be significantly different, and presumably better, than ones for the primitive equations, and/or they must be at least competitive in computational cost. In the case of replacing a rigid lid with a free surface, Dukowicz & Smith (1994) show that there can be a considerable gain in computational efficiency at high resolution in a complex domain with no significant physical difference in the solutions. Marshall et al (1995) use a nonhydrostatic OGCM in the North Pacific and Mediterranean basins, with only a modest multiplication of the computational cost over the primitive equations.

### 3. MODEL SOLUTIONS

The major currents of the oceans are found in all OGCM solutions with climatological wind stress and tracer restoring conditions, and the basic dynamical reasons for their existence are well known [see the theoretical reviews by Veronis (1981) and Young (1987)]. It remains a much harder task, however, to calculate the currents with quantitative accuracy.

Figures 1–3 illustrate the time-averaged currents in an OGCM solution with coarse grid resolution and periodic seasonal forcing with tracer restoring

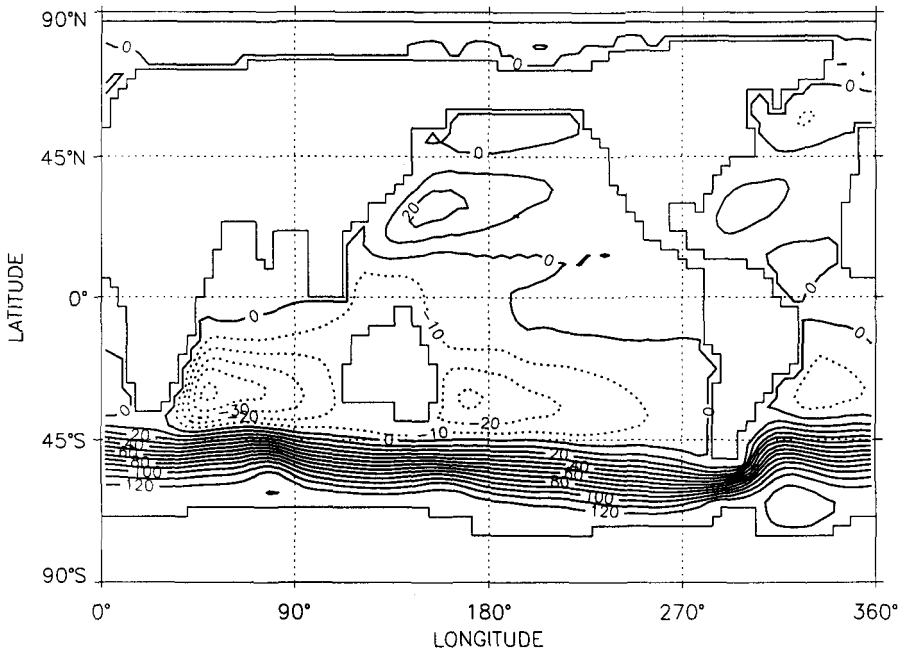


Figure 1 Time-averaged, depth-integrated horizontal transport streamfunction in Sv ( $1 \text{ Sv} = 10^6 \text{ m}^3 \text{ s}^{-1}$ ) in a coarsely resolved OGCM solution. The flow direction is clockwise around maxima. (After Danabasoglu et al 1994.)

conditions. The SGS diffusivities are large enough to prevent any natural variability. The horizontal velocities (Figures 1–2) have a nearly geostrophic momentum balance, augmented in the surface PBL (i.e. Ekman layer) by a SGS turbulent stress divergence. The major currents are

1. the eastward Antarctic Circumpolar Current;
2. the westward, horizontally divergent surface currents in the equatorial Atlantic and Pacific that lie just above eastward equatorial undercurrents;
3. the Indonesian throughflow;
4. the Somali gyre in the western tropical Indian Ocean that occurs mainly during northern-hemisphere summer;
5. the subtropical gyres with western boundary currents in all basins;
6. the subpolar gyres in the north Atlantic and Pacific basins; and

7. the flow into the Greenland-Norwegian Sea from both the Canadian sector of the Arctic and the more southerly Atlantic that converges into a deep-water formation (sinking) region.

These OGCM velocities are everywhere too weak, and the current patterns are too broad compared to reality, consistent with low resolution and high diffusivity. However, the total transports for the currents are similar to observed values, except for a systematic absence of inertial, eddy-forced recirculation in the western part of the wind-driven gyres (see below).

The *meridional overturning circulation* [i.e. in the  $(\phi, z)$  plane, integrated in  $\lambda$ ; see Figure 3a] is much weaker than the geostrophic velocities of the gyres and longitudinal currents. It has

1. tropical wind-driven cells in both hemispheres with equatorial upwelling, subtropical sinking, poleward surface flow (also evident in Figure 2), and equatorward return flow mostly within the pycnocline (i.e. the upper-ocean region with strongly stable density stratification);

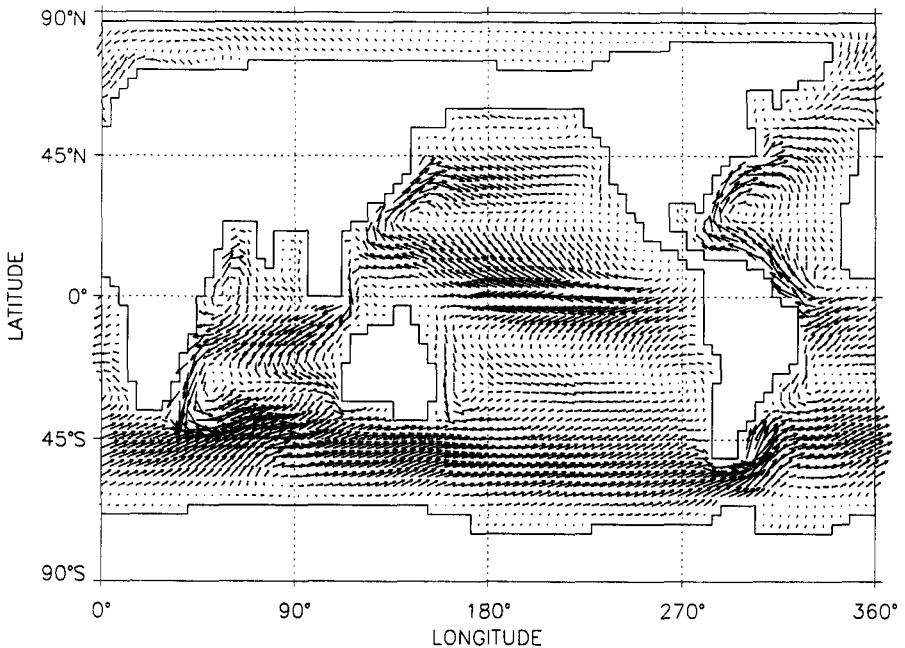
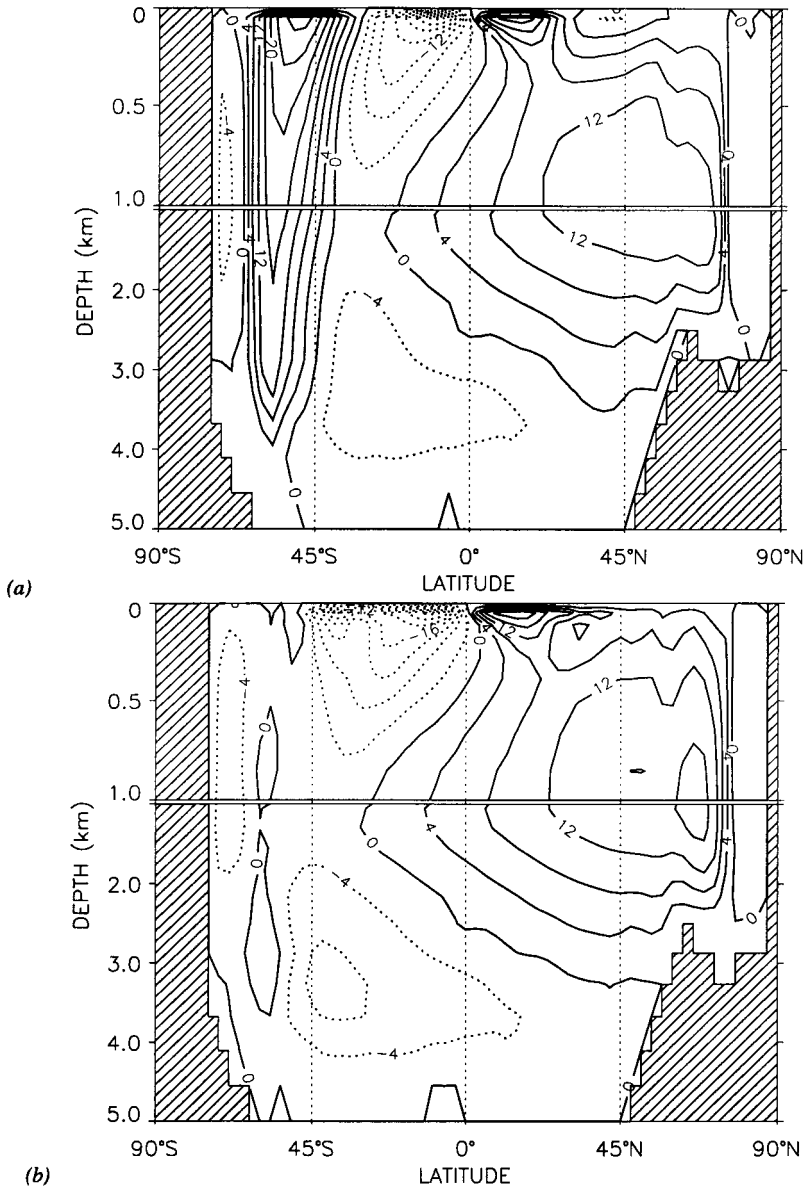


Figure 2 Time-averaged, surface-layer horizontal velocity in a coarsely resolved OGCM solution; the largest vector is  $0.15 \text{ m s}^{-1}$ . (After Danabasoglu et al 1994.)



**Figure 3** (a) Time-averaged, longitude-integrated, meridional-plane transport streamfunction in Sv ( $1 \text{ Sv} = 10^6 \text{ m}^3 \text{ s}^{-1}$ ) in a coarsely resolved OGCM solution. (b) The total tracer transport streamfunction including the parameterized SGS eddy-induced transport. The plotted topographic boundary is the greatest depth found along a latitude line. (After Danabasoglu et al 1994.)

2. wind-driven cells of opposite sign that lie further poleward—a weak one associated with the northern subpolar gyres and a very strong one, sometimes called the *Deacon Cell*, in the Circumpolar Current;
3. a strong buoyancy-driven cell associated with the North Atlantic sinking region; and
4. a weaker buoyancy-driven cell with sinking in the Weddell and Ross Seas near Antarctica and northward flow along the bottom.

The overturning circulation with North Atlantic sinking is referred to as the oceanic *conveyor belt*, for its central role in latitudinal property fluxes; Figure 3 shows its projection on the meridional plane, but it also has a complex three-dimensional structure as it traverses the three major ocean basins. There are pathways of material transport between the cell, with Antarctic sinking and the deepest cell going northward along the bottom into the northern hemisphere, in spite of the apparent interruption by the opposing Deacon Cell; they involve both SGS eddy transport (see below) and northward flow in the deep western boundary currents. The empirical evidence for judging Figure 3*a* is sufficiently uncertain that no strong criticisms of its accuracy can yet be made, apart from the obvious smearing of geographic detail in the coarsely resolved OGCM basins.

In the preceding descriptive taxonomy, and continued below, the circulations are partitioned by wind- or buoyancy-driving, based upon whichever is the essential cause for their existence. In the ocean these causal influences combine inextricably to produce the actual, three-dimensional circulation. For example, wind-driven gyres are largely confined to the pycnocline in the upper ocean, but the existence of the latter is due to the latitudinal difference in buoyancy forcing that causes dense seawater to be carried by convection to great depths in subpolar regions and then move equatorward underneath the shallow, stably stratified light seawater in tropical and middle latitudes.

### 3.1 Wind-Driven Circulations

The wind-driven gyres have a depth-integrated vorticity balance such that the torque applied by the curl of the wind stress approximately balances advection of planetary vorticity (i.e.  $\mathbf{v} \cdot \nabla f$ ), at least for the larger scale circulation over much of the basin. This *Sverdrup balance* is well satisfied in Figure 1 outside the transport-returning, western boundary currents. The boundary currents are controlled by SGS horizontal viscosity here, but more realistically they have an inertial dynamics, as in the fine-resolution, eddy-resolving OGCM solution in Figure 4. The Sverdrup balance can be modified by baroclinic topographic torques, as discussed in Section 2.4 above. Most substantially, however, it is modified by eddy-driven recirculation gyres that greatly enhance

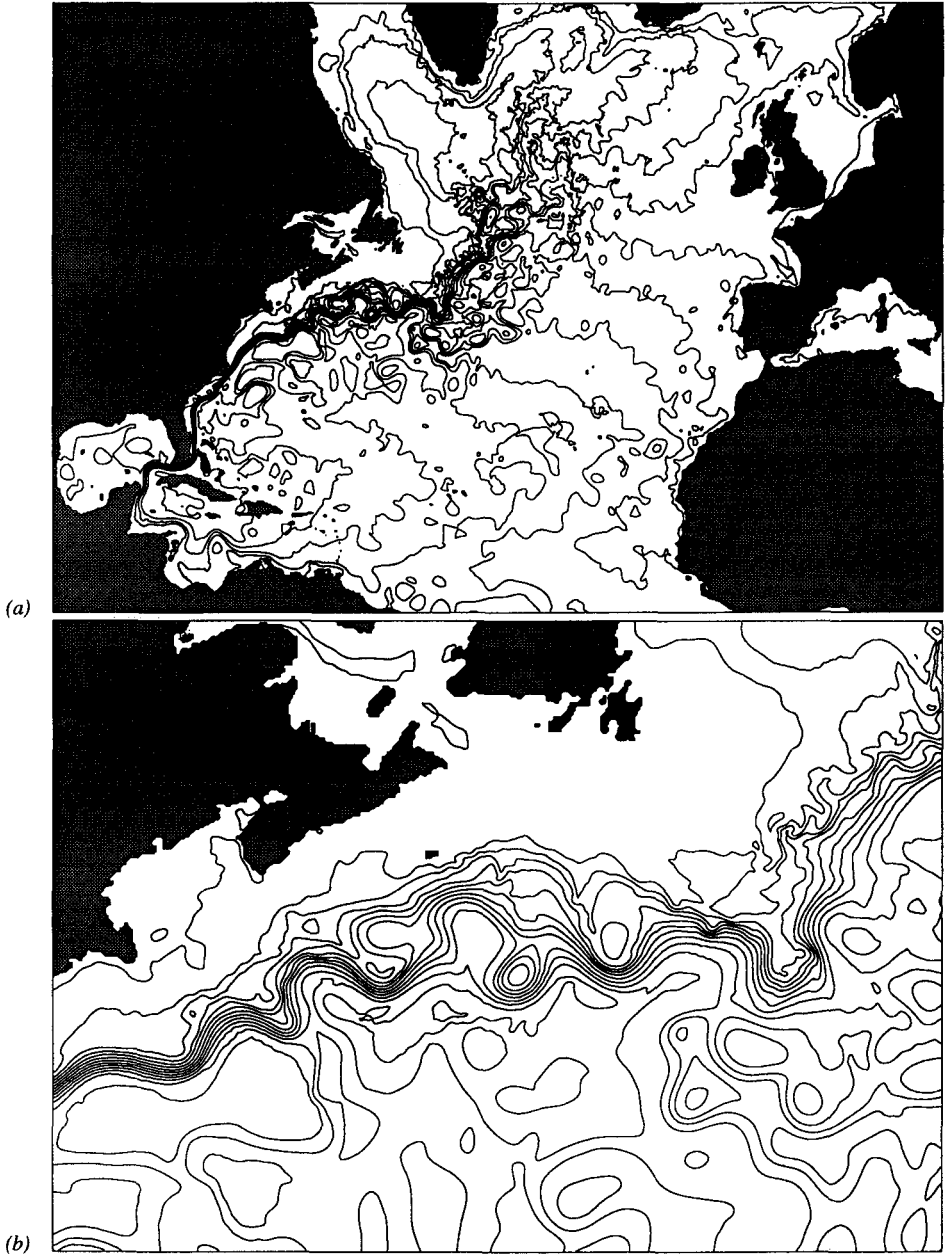


Figure 4 Instantaneous sea-surface height in a finely resolved North Atlantic OGCM solution: (a) full model domain, (b) offshore Gulf Stream region. The contour interval is 0.1 m. (After Bleck et al 1995.)

the gyre transport inside the separating boundary currents (Rhines & Holland 1979, Holland 1985). Evidently the default SGS mesoscale parameterization form of horizontal momentum diffusion is inadequate, for it fails to represent this qualitatively important feature of wind-driven gyres.

A persistently troublesome aspect of OGCM solutions is the western boundary current separation site. In a solution as coarsely resolved as in Figure 1, the issue is moot beyond a general correspondence with the change in sign of the curl of the wind stress (as in Sverdrup balance). In more finely resolved solutions, however, this location is sensitive to lateral stress boundary conditions (Chassignet & Gent 1991, Haidvogel et al 1992); competition between the strength of the wind forcing in adjacent subtropical and subpolar gyres (McWilliams et al 1990, Rhines & Schopp 1991, Verron & Le Provost 1991); inertial, partly ageostrophic, boundary current dynamics (McWilliams et al 1990); the strength of the underlying deep western boundary current driven by buoyancy forcing (Thompson & Schmitz 1989, Spall 1995b); topography (Hurlburt et al 1994, 1995); and various combinations of several of these (Cherniawsky & Holloway 1993). The kinematic constraint associated with isopycnal surfacing (i.e. outcropping) that geostrophically balances an offshore (i.e. separated) current in *pointwise adiabatic* models (without any sources or sinks of material properties; e.g. Parsons 1969, Chassignet & Bleck 1993) seems to largely disappear when nonadiabatic PBL effects are included (Nurser & Williams 1990, Chassignet et al 1995). A recent OGCM solution with an extremely fine horizontal grid spacing of less than 10 km (Bleck et al 1995) achieves a good match for the Gulf Stream separation site (Figure 4), supporting the widespread view that making the boundary layer dynamics sufficiently inertial is particularly important.

The Antarctic Circumpolar Current is driven by an eastward surface wind stress, and unlike other circulations in basins with longitudinal boundaries, this stress cannot be principally balanced in the longitudinal momentum equation by a pressure-gradient force. Instead, the surface stress is approximately balanced by a topographic form stress (see Section 2.4) in a depth integral over the ocean; the vertical momentum flux from top to bottom is accomplished through the *isopycnal form stress* associated with a combination of transient (mesoscale) and standing (time-mean, longitudinally varying) eddies; this is a horizontal pressure force averaged in  $(\lambda, t)$  over a material surface of constant potential density. This dynamical regime has been demonstrated both in idealized, pointwise adiabatic models (McWilliams et al 1978, McWilliams & Chow 1981, Treguier & McWilliams 1990, Wolff et al 1991) and in a nonadiabatic, eddy-resolving OGCM calculation, called the Fine Resolution Antarctic Model (FRAM) (Webb et al 1991, Killworth & Nanneh 1994, Stevens & Ivchenko

1995). Longitudinal isopycnal form stress by geostrophic eddies also implies a latitudinal eddy buoyancy flux; to achieve equilibrium balance in the interior, nearly adiabatic, time- and longitude-averaged buoyancy equation, there must be a mean buoyancy advection balancing the eddy flux divergence,

$$\bar{\mathbf{v}} \cdot \nabla \bar{\rho} \approx -\nabla \cdot \overline{\mathbf{v}'\rho'} \longrightarrow -\mathbf{v}^* \cdot \nabla \bar{\rho}, \quad (3)$$

where the overbar denotes a mean and the prime a fluctuation. The mean (ageostrophic) advecting velocity  $\bar{\mathbf{v}}$  is the overturning Deacon cell in Figure 3a. In an equilibrium balance of this type, there is no net flux of material across the stably stratified isopycnal surfaces. Doos & Webb (1994) show from the FRAM solution that the mean overturning velocity is very much weaker if the  $(\lambda, t)$  average is taken on a surface of constant potential density, rather than constant  $z$ , which is consistent with small net material flux across interior isopycnal surfaces. Analogously, the mesoscale tracer transport parameterization of Gent & McWilliams (1990), formally indicated by the arrow in Equation (3), implies an eddy-induced transport velocity  $\mathbf{v}^*$  that acts to cancel the mean overturning circulation in this situation, and Danabasoglu et al (1994) show that coarse-resolution OGCM solutions with this parameterization have their Deacon Cell nearly canceled (see Figure 3b). In contrast, a parameterization of eddy tracer transport as horizontal diffusion would imply a strongly non-adiabatic flux across the steep isopycnal slopes in this regime. In the integrally adiabatic parameterization, the diffusivity coefficient  $\kappa_1$  expresses the efficiency of eddy transport for a given isopycnal configuration, with  $\mathbf{v}^* \propto \kappa_1$ , and its value strongly influences the total transport through the Drake Passage (Danabasoglu & McWilliams 1995). This confirms the controlling role that geostrophic eddies have in the dynamics of the Antarctic Circumpolar Current.

### 3.2 Buoyancy-Driven Circulations

The geographical patterns of buoyancy forcing differ for heat and fresh water. Tropical heating and polar cooling tend to force a circulation with sinking at high latitudes, whereas tropical excess evaporation (largest somewhat away from the equator) and polar excess precipitation tend to force sinking at low latitudes. This creates the possibility of multiple equilibria with alternative overturning circulation patterns, as first illustrated by Stommel (1961) in a simple box model and subsequently extensively studied in more complex box and two-dimensional (i.e.  $\lambda, z$ ) fluid models (also see Section 3.4 below). In three-dimensional models, the overturning circulation is accompanied by horizontal recirculation with a strong western boundary current and weak interior horizontal flow in the opposite direction (Stommel & Arons 1960); this implies an abyssal mid-latitude cyclonic gyre pattern driven by polar sinking motion.

Colin de Verdiere (1988) and Suginohara & Aoki (1991) solve for the circulation in rectangular, enclosed basins with only thermal forcing, hence a polar-sinking overturning circulation. There is no resulting barotropic flow, and the horizontal gyre patterns are anticyclonic in shallow water and cyclonic in deep water, consistent with the Stommel-Arons scheme. In combination with climatological wind stress forcing (Colin de Verdiere 1989; Salmon 1986, 1990), the buoyancy driving thus strengthens and expands the area of the anticyclonic, subtropical gyre near the surface and does the same for the cyclonic subpolar gyre at depth. Huang (1993) solves the analogous problem with only surface water forcing, using the natural, mass-flux boundary condition rather than a rigid lid with virtual salt forcing. Because of this there is a barotropic response, called the *Goldsborough-Stommel circulation*, whose pattern is similar to the wind-driven subtropical and subpolar gyres but rotating in the reverse direction (also see Huang & Schmitt 1993). The baroclinic gyre here is primarily anticyclonic near the surface, as in the thermally forced problem, even though their overturning circulations are in the opposite sense. It is clear that the interplay between wind, heat, and water forcing allows for a complex set of possible overturning and gyre circulation patterns. A further *hypsometric* influence can overcome the Stommel-Arons circulation: sloping basin sides cause a horizontal expansion and vertical contraction of a rising fluid layer in the interior and, through potential vorticity conservation, induce an anticyclonic abyssal gyre pattern [see Rhines & MacCready (1989) for laboratory flows and Ishizaki (1994) for the North Pacific]. Finally, the purely buoyancy-driven circulation exhibits a sequence of vertically alternating longitudinal jets below the equatorial pycnocline, as are also observed. Their spatial structure in OGCMs is sensitive to the SGS diffusivities (Suginohara & Fukasawa 1988, Suginohara & Aoki 1991, Suginohara et al 1991); thus, the nature of the true small-scale processes associated with this phenomenon remains an open question.

In all of the preceding solutions there is a strong sensitivity to the SGS vertical tracer diffusivity  $\kappa_v$ , as demonstrated by the authors. Bryan (1987) shows an apparent contradiction, in OGCM solutions in an idealized, fully enclosed basin, between having a realistically sharp and shallow pycnocline with small  $\kappa_v$  and a realistically large poleward heat flux with large  $\kappa_v$ . These properties are not governed primarily by the abyssal  $\kappa_v$  distribution (Cummins et al 1990). Salmon (1990) and Salmon & Hollerbach (1991) show that the pycnocline acts as an internal boundary layer whose thickness varies as  $\kappa_v^{1/2}$  and argue that diffusion across isopycnal surfaces is essential to pycnocline structure and dynamics, contrary to earlier *ideal-pycnocline* models with  $\kappa_v = 0$ . This view is confirmed in a tracer budget analysis showing that, if mesoscale tracer transport is integrally adiabatic, then the net top-surface tracer flux into a volume

bounded by an interior iso-tracer surface must be balanced by vertical diffusion across that surface, and that as  $\kappa_v$  decreases the pycnocline (tracer-cline) sharpens approximately so as to maintain the integral flux balance (McWilliams et al 1995). Observations indicate that  $\kappa_v$  typically has a rather small value of  $\mathcal{O}(10^{-5}) \text{ m}^2 \text{ s}^{-1}$  outside the PBL, consistent with the regime of realistically sharp pycnoclines in OGCM solutions. This can be compared with a typical mesoscale isopycnal diffusivity,  $\kappa_i = \mathcal{O}(10^3) \text{ m}^2 \text{ s}^{-1}$ , demonstrating the enormously greater tracer transport efficiency of the latter motions; however, for typical isopycnal slopes of  $\mathcal{O}(10^{-4})$ , the diffusion times are comparable for the two processes— $\mathcal{O}(10^3)$  years on the global scale.

The pycnocline sharpness and poleward heat flux are not controlled entirely by  $\kappa_v$ . Danabasoglu et al (1994) and Boening et al (1995a) show that replacing SGS horizontal tracer diffusion by the integrally adiabatic parameterization both sharpens the pycnocline by eliminating diffusion across its sloping surface and boosts the flux in the northern hemisphere while strongly diminishing the flux across the Circumpolar Current, all of which improve the correspondence with observations. Latitudinal property fluxes are strongly related to the overturning circulation in Figure 3, and these poleward heat flux effects result, respectively, from extending the latitudinal reach of the northern overturning circulation by avoiding false upwelling in the subtropical western boundary current (sometimes called the *Veronis effect*) and from weakening the Deacon Cell (Figure 3b). The influences of grid resolution and horizontal tracer diffusivity on poleward heat flux are assessed in Bryan (1991) for idealized basins, in Beckmann et al (1994a) for the North Atlantic, and in Covey (1995) for global OGCMs. They show that these sensitivities are fairly weak, except in the vicinity of the Circumpolar Current (see above). This remains true even with the onset of mesoscale eddies at finer resolution, due to nearly canceling changes in transport contributions between the eddy flux and large-scale advection; further testing of this conclusion is warranted at even finer resolution (see Section 3.4). Jiang & Fung (1994) show a relatively small sensitivity of the poleward heat transport to global-scale fluctuations in the surface heat flux caused by a partial compensation between changes in the strength of the overturning circulation and the global-scale temperature gradient, whereas Weaver et al (1994) shows strong variations in poleward transport in response to local surface flux anomalies in the North Atlantic. Although the conveyor-belt circulation in Figure 3 involves strong buoyancy forcing, deep convection, and sinking in the North Atlantic, its strength is also influenced by the wind and buoyancy forcing and circumpolar basin geometry in the southern hemisphere (Toggweiler & Samuels 1993a, 1995a; Ishikawa et al 1994; Hughes & Weaver 1994; McDermott 1995). The time scale for a significant response of the overturning circulation to changes

in the buoyancy and wind forcing is rather rapid,  $\mathcal{O}$  (decades) (Suginohara & Fukasawa 1988, Doescher et al 1994, Hughes & Weaver 1994, Jiang & Fung 1994, Danabasoglu et al 1995). This implies that the thermohaline circulation can be a dynamically active participant in decadal variability and abrupt climate transitions, both past and future, in spite of its  $\mathcal{O}(10^3)$ -year time scales for material recirculation and full equilibration.

The processes of ventilation and subduction involve the existence of material pathways from the surface PBL into the interior gyre circulation in the stably stratified pycnocline by a combination of downward Ekman-layer pumping (vertical velocity driven by the curl of the wind stress) and horizontal flow through the vertically cycling PBL. Using an ideal-pycnocline model based on Ekman pumping, Luyten et al (1983) categorize different regions of the subtropical gyre by their accessibility to ventilation. Cox & Bryan (1984) in an OGCM solution without eddies and Cox (1985, 1987) in solutions with eddies show that this categorization is an approximately valid one, albeit with significantly nonconservative changes in the tracers along large-scale trajectories. Recent analyses by Spall (1995a), New et al (1995), New & Bleck (1995), and Williams et al (1995) indicate that the horizontal flow through the PBL is the dominant pathway and that most of the subduction occurs in early spring when the PBL rapidly shrinks. Some of the subducted seawater moves out of the subtropical gyre to supply the equatorial undercurrent and upwell on the equator, as indicated in the tropical overturning circulation in Figure 3 (Liu et al 1994, McCreary & Lu 1994).

### 3.3 Tracers

Much more attention has been paid to potential temperature than to other tracers in OGCM solutions, both because it is the dominant contributor to density, hence to circulation, and because its boundary condition and interior distribution are relatively better known. Its primary deficiencies in OGCM solutions forced by restoring conditions have been an overly diffuse thermocline and an abyssal warm bias, both of which are much improved with the integrally adiabatic mesoscale tracer transport parameterization (see above). The other dynamically relevant tracer, salinity, persistently has an abyssal fresh bias in solutions with restoring conditions (Bryan & Lewis 1979), which is not readily corrected by variations in the SGS transport (Danabasoglu & McWilliams 1995). Not uncommonly, therefore, the climatological values for  $S$  have been elevated in the restoring condition in subpolar deep-water formation regions, rationalized by suspicions about observational bias and underestimation of the effects of brine rejection during wintertime sea ice formation (e.g. Cox 1989, England 1993); however, Toggweiler & Samuels (1995b) argue that such an enhancement near Antarctica is inconsistent with other tracer evidence. Other modifications in

the surface buoyancy forcing can also yield solutions without this bias (e.g. Maier-Reimer et al 1993). Because of uncertainties in surface water flux, both as observed and as implied by restoring conditions (see Section 2.3 above), no strong conclusions about OGCM dynamical accuracy can yet be drawn from its  $S$  distributions.

Other, nondynamical tracers also suffer from poorly known boundary conditions, interior distributions, and/or biogeochemical reactions. Because hydrographic observations provided the earliest inferential basis for the general circulation, a widespread belief among oceanographers has been that tracers would prove very useful in judging OGCM solutions, particularly if many different tracers, with distinct sources and sinks, were used. Most likely this will come to pass, perhaps most definitively within a framework of data assimilation into OGCM solutions, but it seems premature to make a critical assessment. Recent pioneering calculations for particular tracers include those by Toggweiler et al (1989) and Toggweiler & Samuels (1993b) for pre-industrial and anthropogenic radiocarbon, Najjar et al (1992) and Sarmiento et al (1993) for nutrients, Maier-Reimer (1993) for a suite of pre-industrial tracers, England et al (1994) and Robitaille & Weaver (1995) for anthropogenic freons, and Sarmiento (1983) and Jia & Richards (1995) for anthropogenic tritium/helium.

### 3.4 *Variability*

The variability of the general circulation is still largely unknown, because direct observations are spatially sparse and span only a few decades, indirect paleoclimatic evidence is quite fragmentary, and relevant modeling studies are in their infancy. The atmospheric forcing has broad bandwidth in its wavenumber-frequency spectrum, and it is likely that the spectrum of oceanic response is also broadband but shifted towards lower frequencies because of its characteristically slower dynamical rates (Hasselmann 1976). The strongest forcing component is the annual cycle, which causes large variation in upper-ocean tracer fields, currents, and tracer transports (e.g. Boening et al 1991, Boening & Herrmann 1994). The most evident natural variability in the oceans is the geostrophic mesoscale eddies generated primarily by instability of the wind-driven currents (e.g. Holland 1985, Semtner & Chervin 1992). Geostrophic eddies also have a broadband spectrum, which may extend beyond the mesoscale into the large-scale, low-frequency range of the general circulation (e.g. McCalpin & Haidvogel 1995). Finally, there are many recent examples of natural variability in the buoyancy driven circulation, which thus far have been realized only as nearly periodic, hence narrowband, oscillations with periods from decades to millennia (e.g. Weaver et al 1993). From the viewpoint that the SGS diffusivity is a bifurcation parameter, we can speculate that this is perhaps

because of their marginal supercriticality in the coarsely resolved calculations to date. There are also examples of periodic solutions in adiabatic, steadily wind-driven basin models (Holland & Lin 1975, Jiang et al 1995) near their critical points.

Thermohaline variability has been investigated mostly by using mixed tracer boundary conditions (Section 2.3) or else with an incremental, broadband stochastic component to the buoyancy forcing. If there are natural modes of oscillation implicit in a given model formulation, then stochastic forcing can expose the modes that are least damped, whether they lie just below or above a critical threshold for linear instability about the time-mean circulation. With these boundary conditions multiple equilibria often exist in OGCMs, and an issue of particular interest is the possibility of a *polar halocline catastrophe*, where the presently dominant mode of thermohaline circulation is unstable and the solution evolves to a much weaker overturning circulation pattern (Bryan 1986, Marotzke & Willebrand 1991, Hughes & Weaver 1994, Power et al 1994). These boundary conditions also permit spontaneous oscillations, which at present appear to fall into three broad groupings ordered by period:

1. decadal oscillations that involve gyre advection of buoyancy anomalies in an essential way (e.g. Weaver & Sarachik 1991, Huang 1993, Weisse et al 1994, Greatbatch & Zhang 1995, Chen & Ghil 1995, Yin & Sarachik 1995, Cai et al 1995);
2. centennial *loop* oscillations that involve advection of buoyancy anomalies primarily by the overturning circulation (Mikolajewicz & Maier-Reimer 1990, Winton & Sarachik 1993, Barnett et al 1994, Pierce et al 1995a); and
3. millennial *flushing* or *deep-decoupling* oscillations with long intervals of SGS diffusive destabilization of the abyssal ocean punctuated by much briefer convective events (e.g. Weaver et al 1993, Winton & Sarachik 1993, Huang 1994).

There is at least some observational evidence for decadal oscillations in the North Atlantic subpolar gyre. The various bifurcations associated with these instabilities and oscillations are quite sensitive to many aspects of the surface tracer flux conditions; in particular, it is quite important how the flux changes as the ocean circulation changes, which involves climate feedbacks that cannot be settled entirely within an OGCM. Through investigations of alternative surface conditions, the preponderance of opinion has recently swung towards a lesser fragility, and possibly lesser natural variability, of the thermohaline circulation (Zhang et al 1993, Mikolajewicz & Maier-Reimer 1994, Tziperman et al 1994, Power et al 1994, Pierce et al 1995b). However, these issues are far from being resolved.

Analogously, variability of the general circulation occurs in response to variability in the surface wind stress. In OGCM solutions the strongest components of the extra-topical response are barotropic and baroclinic Rossby waves, both on the mesoscale and on larger scales (Barnier & LeProvost 1989, Large et al 1991, Jacobs et al 1994, Milliff et al 1995). In an idealized calculation, Seidov & Marushkevich (1992) show the possibility of *transient rectification* where the transient currents provide a time-mean eddy momentum stress that modifies the steadily forced component of the mean circulation, in regions where the waves are trapped by the mean circulation and basin geometry. This effect has not yet been demonstrated in an OGCM solution.

Eddy-resolving OGCM solutions have thus far been calculated only for intervals of  $\mathcal{O}(\text{decades})$ , which precludes their applicability to issues of low-frequency variability and equilibrium thermohaline circulation. Instead, the purposes are to examine how geostrophic eddies contribute to the dynamical balance of the general circulation on a decadal time scale and, indirectly, to assess model skill through comparisons of eddy properties with observations. Most solutions are obtained within single basins because of the smaller computational grid required to achieve a given resolution and the more rapid equilibration time (albeit with substantial control by the conditions imposed at the open-water boundaries). Conspicuous exceptions are the pioneering global solutions of Semtner & Chervin (1988, 1992) and, with as yet only preliminary results, those of Dukowicz et al (1993) and Dukowicz & Smith (1994). Holland & Lin (1975) show the first eddy-resolving solutions for adiabatic, wind-driven circulation in an idealized basin, and many subsequent investigations have been made for this idealized problem (see the reviews in Holland 1985 and Young 1987). Early eddy-resolving OGCM solutions were obtained by Semtner & Mintz (1977) and by Cox (1985, 1987). Perhaps the most systematic body of research has been in the North Atlantic basin, under the auspices of the Community Modeling Effort (CME) (e.g. Beckmann et al 1994a,b; Bryan et al 1995; Boening et al 1995b; EP Chassignet, personal communication). Other eddy-resolving OGCM solutions are for the Antarctic Circumpolar region (FRAM: Webb et al 1991, Stevens & Killworth 1992) and the North Pacific (Hurlburt et al 1994). The most challenging issue for eddy-resolving models is their sensitivity to the horizontal grid resolution. Present evidence indicates that the grid scale must be at least as small as  $\mathcal{O}(10)$  km in middle and high latitudes, judged by its influences on eddy variance and boundary-current behavior (Barnier et al 1991, Boening & Budich 1992, Beckmann et al 1994a, Bleck et al 1995); however, no convergence with resolution has been demonstrated. Mesoscale eddies do indeed contribute substantially to the dynamical balances of the general circulation, as could be anticipated from the significant control exerted by their

SGS parameterizations in more coarsely resolved models. It is still uncertain, however, in what ways the largest-scale features of the circulation, such as the Circumpolar Current and conveyor belt in Figures 1–3, have mesoscale contributions that cannot be adequately represented in SGS parameterizations. It is certain, though, that this question cannot be answered except through eddy-resolving OGCM solutions and that the strongest currents are quite different in coarsely and finely resolved solutions (cf Figures 2 & 4).

#### 4. SUMMARY AND PROSPECTS

Models of the oceanic general circulation are currently in a phase of rapid development and expanding utilization. Within the range of legitimate choices for model formulation and boundary conditions, surveyed above, present model solutions do seem to encompass the major features of the circulation as observed. In the coming decades the challenge will be to narrow and refine the modeling choices and reduce observational uncertainties, with mutual consistency. The biggest surprises are likely to come in weaning the ocean model from its specified, or at least strongly constrained, surface boundary conditions, as it assumes its proper, more fundamental role in the dynamics of the Earth's climate system.

#### ACKNOWLEDGMENTS

Many of the scientists cited in this review made useful suggestions about their own contributions to OGCMs when asked, and I hope that they will find the discussion here fair and accurate. I appreciate the help of my colleague Gokhan Danabasoglu in preparing Figures 1–3, and I am grateful to Rainer Bleck for preparation of Figure 4.

Any *Annual Review* chapter, as well as any article cited in an *Annual Review* chapter, may be purchased from the Annual Reviews Preprints and Reprints service.  
1-800-347-8007; 415-259-5017; email: arpr@class.org

#### Literature Cited

- Armi L. 1978. Some evidence for boundary mixing in the deep ocean. *J. Geophys. Res.* 83:1971–79
- Armi L, Farmer DM. 1988. The flow of Mediterranean and Atlantic water through the strait of Gibraltar. *Prog. Oceanog.* 21:1–106
- Barnett TP, Chu M, Wilde R, Mikolajewicz U. 1994. Low frequency ocean variability induced by stochastic forcing of various colors. In *Decade to Century Time scales of Climate Variability*, ed. DG Martinson, K Bryan, M Ghil, MM Hall, TR Karl, et al. Washington, DC: Natl. Acad. Sci. In press
- Barnier B, Hua BL, LeProvost C. 1991. On the catalytic role of high baroclinic modes in eddy-driven large-scale circulations. *J. Phys. Oceanogr.* 21:976–97
- Barnier B, LeProvost C. 1989. General circu-

- lation of the mid-latitude ocean: coupled effects of variable wind stress forcing and topography roughness on the mean circulation. In *Mesoscale/Synoptic Structures in Geophysical Turbulence*, ed. JC Nihoul, BM Jamart, pp. 387–405. Amsterdam: Elsevier
- Barnier B, Siefridt L, Marchesio P. 1995. Thermal forcing for a global ocean circulation model using a three-year climatology of ECMWF analyses. *J. Mar. Syst.* 6:363–80
- Beckmann A, Boening CW, Brugge B, Stammer D. 1994b. On the generation and role of eddy variability in the central North Atlantic Ocean. *J. Geophys. Res.* 99:20,381–91
- Beckmann A, Boening CW, Koeberle C, Willebrand J. 1994a. Effects of increased horizontal resolution in a simulation of the North Atlantic Ocean. *J. Phys. Oceanogr.* 24:326–44
- Bleck R, Chassignet E. 1994. Simulating the oceanic circulation with isopycnic-coordinate models. In *The Oceans: Physical-Chemical Dynamics and Human Impact*, ed. SK Majumdar, EW Miller, pp. 17–39. Easton, PA: Penn. Acad. Sci.
- Bleck R, Dean S, O'Keefe M, Sawdey A. 1995. A comparison of data-parallel and message-passing versions of the Miami Isopycnic coordinate Ocean Model. *Parallel Computing Submitted*
- Boening CW. 1989. Influences of a rough bottom topography on flow kinematics in an eddy resolving model. *J. Phys. Oceanogr.* 19:77–97
- Boening CW, Bryan FO, Holland WR, Doescher R. 1995b. Thermohaline circulation and poleward heat transport in a high-resolution model of the North Atlantic. *J. Phys. Oceanogr.* Submitted
- Boening CW, Budich RG, Reinhard G. 1992. Eddy dynamics in a primitive equation model: sensitivity to horizontal resolution and friction. *J. Phys. Oceanogr.* 22:361–81
- Boening CW, Doescher R, Budich RG. 1991. Seasonal transport variation in the western subtropical North Atlantic: experiments with an eddy resolving model. *J. Phys. Oceanogr.* 21:1271–89
- Boening CW, Herrmann P. 1994. Annual cycle of poleward heat transport in the ocean: results from high resolution modeling of the North and Equatorial Atlantic. *J. Phys. Oceanogr.* 24:326–44
- Boening CW, Holland WR, Bryan FO, Danabasoglu G, McWilliams JC. 1995a. An overlooked problem in model simulations of the thermohaline circulation and heat transport in the Atlantic Ocean. *J. Climate* 8:515–23
- Bretherton FP, Haidvogel DB. 1976. Two-dimensional turbulence above topography. *J. Fluid Mech.* 78:129–54
- Bretherton FP, Karweit M. 1975. Mid-ocean mesoscale modeling. In *Numerical Models of Ocean Circulation*, ed. RO Reid, pp. 237–49. Washington, DC: Natl. Acad. Sci.
- Bryan FO. 1986. High-latitude salinity effects and interhemispheric thermohaline circulations. *Nature* 323:301–4
- Bryan FO. 1987. Parameter sensitivity of primitive equation ocean general circulation models. *J. Phys. Oceanogr.* 17:970–85
- Bryan FO, Boening CW, Holland WR. 1995. On the mid-latitude circulation in a high-resolution model of the North Atlantic. *J. Phys. Oceanogr.* 25:289–305
- Bryan K. 1969. A numerical method for the study of the circulation of the world ocean. *J. Comput. Phys.* 4:347–76
- Bryan K. 1984. Accelerating the convergence to equilibrium of ocean-climate models. *J. Phys. Oceanogr.* 14:666–83
- Bryan K. 1991. Poleward heat transport in the ocean: a review of a hierarchy of models of increasing resolution. *Tellus* 43A:104–15
- Bryan K, Cox M. 1967. A numerical investigation of the oceanic general circulation. *Tellus* 19:54–80
- Bryan K, Cox M. 1968. A nonlinear model of an ocean driven by wind and differential heating. I. Description of the three-dimensional velocity and density fields. II. An analysis of the heat, vorticity, and energy balance. *J. Atmos. Sci.* 25:945–78
- Bryan K, Lewis LJ. 1979. A water mass model of the world ocean. *J. Geophys. Res.* 84:2503–17
- Cai W, Greatbatch RJ, Zhang S. 1995. Interdecadal variability in an ocean model driven by a small, zonal redistribution of the surface buoyancy flux. *J. Phys. Oceanogr.* In press
- Charney JG. 1971. Geostrophic turbulence. *J. Atmos. Sci.* 28:1087–95
- Chassignet EP, Bleck R. 1993. The influence of layer outcropping on the separation of boundary currents. Part I: The wind-driven experiment. *J. Phys. Oceanogr.* 23:1485–507
- Chassignet EP, Bleck R, Rooth CGH. 1995. The influence of layer outcropping on the separation of boundary currents. Part II: The wind- and buoyancy-driven experiments. *J. Phys. Oceanogr.* In press
- Chassignet EP, Gent PR. 1991. The influence of boundary conditions on mid latitude jet separation in ocean numerical models. *J. Phys. Oceanogr.* 21:1290–99
- Chen F, Ghil M. 1995. Interdecadal variability of the thermohaline circulation and high-latitude surface fluxes. *J. Phys. Oceanogr.* Submitted
- Cherniawsky J, Holloway G. 1993. On western boundary current separation in an upper

- ocean general circulation model of the North Pacific. *J. Geophys. Res.* 98:22,843–53
- Colin de Verdiere A. 1988. Buoyancy driven planetary flows. *J. Mar. Res.* 46:215–65
- Colin de Verdiere A. 1989. On the interaction of wind and buoyancy driven gyres. *J. Mar. Res.* 47:595–633
- Colin de Verdiere A, Schopp R. 1994. Flows in a rotating spherical shell: the equatorial case. *J. Fluid Mech.* 276:233–60
- Covey C. 1995. Global ocean circulation and equator-pole heat transport as a function of ocean GCM resolution. *Climate Dyn.* In press
- Cox MD. 1975. A baroclinic numerical model of the ocean: preliminary results. In *Numerical Models of Ocean Circulation*, ed. RO Reid, pp. 107–18. Washington, DC: Natl. Acad. Sci.
- Cox MD. 1985. An eddy-resolving numerical model of the ventilated thermocline. *J. Phys. Oceanogr.* 15:1312–24
- Cox MD. 1987. An eddy-resolving numerical model of the ventilated thermocline: time dependence. *J. Phys. Oceanogr.* 17:1044–56
- Cox MD. 1989. An idealized model of the world ocean. Part I: The global scale water masses. *J. Phys. Oceanogr.* 19:1730–52
- Cox MD, Bryan K. 1984. A numerical model of the ventilated thermocline. *J. Phys. Oceanogr.* 14:674–87
- Cummins PF. 1991. The deep water stratification of ocean general circulation models. *Atmosphere-Ocean* 29:563–75
- Cummins PF, Holloway G, Gargett AE. 1990. Sensitivity of the GFDL oceanic general circulation model to a parameterization of vertical diffusion. *J. Phys. Oceanogr.* 20:817–30
- Danabasoglu G, McWilliams JC. 1995. Sensitivity of the global ocean circulation to parameterizations of mesoscale tracer transports. *J. Climate*. In press
- Danabasoglu G, McWilliams JC, Gent PR. 1994. The role of mesoscale tracer transports in the global ocean circulation. *Science* 264:1123–26
- Danabasoglu G, McWilliams JC, Large WG. 1995. Approach to equilibrium in global ocean models. *J. Climate*. Submitted
- Dietrich DE, Marietta MG, Roache PJ. 1987. An ocean modeling system with turbulent boundary layers and bottom topography: Numerical description. *Int. J. Numer. Methods Fluids* 7:833–55
- Dietrich DE, Roache PJ, Marietta MG. 1990. Convergence studies with the Sandia Ocean Modeling System. *Int. J. Numer. Methods Fluids* 11:127–50
- Doescher R, Boening CW, Herrmann P. 1994. Response of meridional overturning and heat transport in the North Atlantic to changes in thermohaline forcing in northern latitudes; a model study. *J. Phys. Oceanogr.* 24:2306–20
- Doos K, Webb DJ. 1994. The Deacon Cell and other meridional cells of the southern ocean. *J. Phys. Oceanogr.* 24:429–42
- Dukowicz JK, Smith RD. 1994. Implicit free-surface method for the Bryan-Cox-Semtner ocean model. *J. Geophys. Res.* 99:7991–8014
- Dukowicz JK, Smith RD, Malone RC. 1993. A reformulation and implementation of the Bryan-Cox-Semtner ocean model on the Connection Machine. *J. Atmos. Oceanogr. Tech.* 10:195–208
- Ebby M, Holloway G. 1994a. Sensitivity of a large-scale ocean model to a parameterization of topographic stress. *J. Phys. Oceanogr.* 24:2577–88
- Ebby M, Holloway G. 1994b. Grid transform for incorporating the Arctic in a global ocean model. *Climate Dyn.* 10:241–47
- England MH. 1993. Representing the global-scale water masses in ocean general circulation models. *J. Phys. Oceanogr.* 23:1523–52
- England MH, Garcon V, Minster JF. 1994. Chlorofluorocarbon uptake in a world ocean model. I. Sensitivity to surface gas forcing. *J. Geophys. Res.* 99:25,215–33
- Ezer T, Mellor GL. 1994. Diagnostic and prognostic calculations of the North Atlantic circulation and sea level using a sigma coordinate ocean model. *J. Geophys. Res.* 99:14,159–71
- Gargett AE, Holloway G. 1992. Sensitivity of the GFDL ocean model to different diffusivities for heat and salt. *J. Phys. Oceanogr.* 22:1158–77
- Garrett C. 1991. Marginal mixing theories. *Atmosphere-Ocean* 29:313–39
- Garwood RW, Isakari SM, Gallacher PC. 1994. Thermobaric convection. In *The Polar Oceans and Their Role in Shaping the Global Environment*, ed. OM Johannessen, RD Muench, JE Overland, Geophys. Monogr. 85, pp. 199–209. Washington, DC: Am. Geophys. Union
- Gent PR, McWilliams JC. 1990. Isopycnal mixing in ocean circulation models. *J. Phys. Oceanogr.* 20:150–55
- Gent PR, Willebrand J, McDougall TJ, McWilliams JC. 1995. Parameterizing eddy-induced tracer transports in ocean circulation models. *J. Phys. Oceanogr.* 25:463–74
- Gill A, Bryan K. 1971. Effects of geometry on the circulation of a three-dimensional southern-hemisphere ocean model. *Deep-Sea Res.* 18:685–721
- Greatbatch RJ, Zhang S. 1995. An interdecadal oscillation in an idealized ocean basin forced by constant heat flux. *J. Climate* 8:81–91
- Haidvogel DB, Bryan FO. 1992. Ocean gen-

- eral circulation modeling. In *Climate System Modeling*, ed. K Trenberth, pp. 371–412. New York: Oxford Univ. Press
- Haidvogel DB, Curchitser E, Iskandarani M, Hughes R, Taylor M. 1995. Global modeling of the ocean and atmosphere using the spectral element method. *Atmosphere-Ocean*. In press
- Haidvogel DB, McWilliams JC, Gent PR. 1992. Boundary current separation in a quasi-geostrophic, eddy-resolving ocean circulation model. *J. Phys. Oceanogr.* 22:882–902
- Han Y-J. 1984. A numerical world ocean general circulation model. Part II. A baroclinic experiment. *Dyn. Atmos. Oceans* 8:141–72
- Haney R. 1971. Surface thermal boundary condition of ocean circulation models. *J. Phys. Oceanogr.* 1:145–67
- Hasselmann K. 1976. Stochastic climate models. Part I: Theory. *Tellus* 28:473–85
- Hirst AC, Godfrey JS. 1993. The role of Indonesian throughflow in a global ocean GCM. *J. Phys. Oceanogr.* 23:1057–86
- Holland WR. 1971. Ocean tracer distributions. Part I: A preliminary numerical experiment. *Tellus* 23:371–92
- Holland WR. 1985. Simulation of mid-ocean mesoscale ocean variability in mid-latitude gyres. *Adv. Geophys.* 28:479–523
- Holland WR, Harrison DE, Semtner A. 1983. Eddy-resolving numerical models of large-scale circulation. In *Eddies in Marine Sciences*, ed. AR Robinson, pp. 379–403. Heidelberg: Springer-Verlag
- Holland WR, Lin LB. 1975. On the generation of mesoscale eddies and their contribution to the oceanic general circulation. I. A preliminary numerical experiment. II. A parameter study. *J. Phys. Oceanogr.* 5:642–69
- Holloway G. 1992. Representing topographic stress for large-scale ocean models. *J. Phys. Oceanogr.* 22:1033–46
- Huang RX. 1993. Real freshwater flux as a natural boundary condition for the salinity balance and thermohaline circulation forced by evaporation and precipitation. *J. Phys. Oceanogr.* 23:2428–46
- Huang RX. 1994. Thermohaline circulation: energetics and variability in a single-hemisphere basin model. *J. Geophys. Res.* 99:12,471–85
- Huang RX, Schmitt RW. 1993. The Goldsborough-Stommel circulation of the world oceans. *J. Phys. Oceanogr.* 23:1277–84
- Hughes TMC, Weaver AJ. 1994. Multiple equilibria of an asymmetric two-basin ocean model. *J. Phys. Oceanogr.* 24:619–37
- Hurlburt HE, Hogan PJ, Metzger EJ, Schmitz WJ, Wallcraft AJ. 1995. Dynamics of eddy-resolving models of the Pacific Ocean and the Sea of Japan. In *Workshop on Numerical Prediction of Oceanic Variations*, pp. 51–57. Tokyo: Sci. Technol. Agency and Jpn. Meteorol. Agency
- Hurlburt HE, Wallcraft AJ, Schmitz WJ, Metzger EJ, Hogan PJ. 1994. Dynamics of the Kuroshio/Oyashio current system using eddy-resolving models of the North Pacific Ocean. *J. Geophys. Res.* In press
- Ishikawa I, Yamanaka Y, Suginozono N. 1994. Effects of presence of a circumpolar region on buoyancy-driven circulation. *J. Oceanogr.* 50:247–63
- Ishizaki H. 1994. A simulation of the abyssal circulation in the North Pacific Ocean. Part I: Flow field and comparison with observations. Part II: Theoretical rationale. *J. Phys. Oceanogr.* 24:1921–54
- Jacobs GA, Hurlburt HE, Kindle JC, Metzger EZ, Mitchell JL, et al. 1994. Decadal-scale trans-Pacific propagation and warming effects of an El Niño anomaly. *Nature* 370:360–63
- Jia Y, Richards KJ. 1995. Tritium distributions in anisopycnic model of the North Atlantic. *J. Geophys. Res.* Submitted
- Jiang S, Jin FF, Ghil M. 1995. Multiple equilibria, periodic, and aperiodic solutions in a wind-driven, double-gyre, shallow-water model. *J. Phys. Oceanogr.* 25:764–86
- Jiang XJ, Fung I. 1994. Ocean response to surface heat anomalies. *J. Climate* 7:783–91
- Killworth PD, Nanneh MN. 1994. Isopycnal momentum budget of the Antarctic Circumpolar Current in the Fine Resolution Antarctic Model. *J. Phys. Oceanogr.* 24:1201–23
- Kraus EB, Turner S. 1967. A one-dimensional model of the seasonal thermocline. II: The general theory and its consequences. *Tellus* 19:98–106
- Large WG, Holland WR, Evans JC. 1991. Quasi-geostrophic ocean response to real wind forcing: the effects of temporal smoothing. *J. Phys. Oceanogr.* 21:998–1017
- Large WG, McWilliams JC, Doney SC. 1994. Oceanic vertical mixing: a review and a model with a non-local K-profile boundary layer parameterization. *Rev. Geophys.* 32:363–403
- Leonard BP. 1979. A stable and accurate convective modelling procedure based on quadratic upstream interpolation. *Comput. Methods Appl. Mech. Eng.* 19:59–98
- Liu Z, Philander SGH, Pacanowski RC. 1994. A GCM study of tropical-subtropical upper-ocean water exchange. *J. Phys. Oceanogr.* 24:2606–23
- Lunkeit F, Sausen R, Oberhuber JM. 1995. Climate simulations with a global coupled atmosphere-ocean model ECHAM2/OPYC.

- Climate Dyn.* In press
- Luyten JR, Pedlosky J, Stommel H. 1983. The ventilated thermocline. *J. Phys. Oceanogr.* 13:292-309
- Maier-Reimer E. 1993. Geochemical cycles in an ocean general circulation model. Preindustrial tracer distributions. *Global Biogeochem. Cycles* 7:645-77
- Maier-Reimer E, Mikolajewicz, Hasselmann K. 1993. Mean circulation of the Hamburg LSG OGCM and its sensitivity to thermohaline surface forcing. *J. Phys. Oceanogr.* 23:731-57
- Marotzke J, Willebrand J. 1991. Multiple equilibria of the global thermohaline circulation. *J. Phys. Oceanogr.* 21:1372-85
- Marshall J. 1981. On the parameterization of geostrophic eddies in the ocean. *J. Phys. Oceanogr.* 11:257-71
- Marshall J, Adcroft A, Hill C, Perelman L. 1995. Hydrostatic, quasi-hydrostatic, and non-hydrostatic ocean modeling. *J. Geophys. Res.* Submitted
- McCalpin JD, Haidvogel DB. 1995. Phenomenology of the low-frequency variability in a reduced-gravity, quasigeostrophic double-gyre model. *J. Phys. Oceanogr.* Submitted
- McCreary J, Lu P. 1994. Interaction between the subtropical and equatorial ocean circulations: the subtropical cell. *J. Phys. Oceanogr.* 24:466-97
- McDermott D. 1995. The regulation of northern overturning by southern hemisphere winds. *J. Phys. Oceanogr.* Submitted
- McWilliams JC, Chow JHS. 1981. Equilibrium geostrophic turbulence: I. A reference solution in a  $\beta$ -plane channel. *J. Phys. Oceanogr.* 11:921-49
- McWilliams JC, Danabasoglu G, Gent PR. 1995. Tracer budgets in the warm water sphere. *Tellus.* In Press
- McWilliams JC, Holland WR, Chow JHS. 1978. A description of numerical Antarctic Circumpolar Currents. *Dyn. Atmos. Oceans* 2:213-91
- McWilliams JC, Norton NJ, Gent PR, Haidvogel DB. 1990. A linear balance model of wind-driven, mid-latitude ocean circulation. *J. Phys. Oceanogr.* 20:1349-78
- Mellor G, Yamada T. 1982. Development of a turbulence closure model for geophysical fluid problems. *Rev. Geophys. Space Phys.* 20:851-75
- Mikolajewicz U, Maier-Reimer E. 1990. Internal secular variability in an ocean general circulation model. *Climate Dyn.* 4:145-56
- Mikolajewicz U, Maier-Reimer E. 1994. Mixed boundary conditions in ocean general circulation models and their influence on the stability of the model's conveyor belt. *J. Geophys. Res.* 99:22,633-44
- Milliff RF, Large WG, Holland WR, McWilliams JC. 1995. The general-circulation response of a high-resolution North Atlantic Ocean model to synthetic-scatterometer winds. *J. Phys. Oceanogr.* Submitted
- Munk WH, Palmen E. 1951. Note on the dynamics of the Antarctic Circumpolar Current. *Tellus* 3:53-55
- Najjar RG, Sarmiento JL, Toggweiler JR. 1992. Downward transport and fate of organic matter in the ocean: simulations with a general circulation model. *Global Biogeochem. Cycles* 6:45-76
- New AL, Bleck R. 1995. An isopycnic model study of the North Atlantic. Part 2: Interdecadal variability of the sub-tropical gyre. *J. Physical Oceanogr.* In press
- New AL, Bleck R, Jia Y, Marsh R, Huddleston M, Barnard S. 1995. An isopycnic model study of the North Atlantic. Part 1: Model experiment. *J. Physical Oceanogr.* In press
- Norton NJ, McWilliams JC, Gent PR. 1986. A numerical model of the Balance Equations in a periodic domain and an example of balanced turbulence. *J. Comput. Phys.* 67:439-71
- Nurser AJG, Williams RG. 1990. Cooling Parson's model of the separated Gulf Stream. *J. Phys. Oceanogr.* 20:1974-79
- Owens WB, Bretherton FP. 1978. A numerical study of mid-ocean mesoscale eddies. *Deep-Sea Res.* 25:1-14
- Pacanowski R, Philander G. 1981. Parameterization of vertical mixing in numerical models of tropical oceans. *J. Geophys. Res.* 11:1443-51
- Parsons AT. 1969. A two-layer model of Gulf Stream separation. *J. Fluid Mech.* 39:511-28
- Pierce DW, Barnett TP, Mikolajewicz U. 1995a. On the competing roles of heat and fresh water flux in forcing thermohaline oscillations. *J. Phys. Oceanogr.* In press
- Pierce DW, Kim KY, Barnett TP. 1995b. Variability of the thermohaline circulation in an ocean general circulation model coupled to an atmospheric energy balance model. *J. Phys. Oceanogr.* In press
- Pinardi N, Rosati A, Pacanowski RC. 1995. The sea surface pressure formulation of rigid lid models. Implications for altimetric data assimilation studies. *J. Mar. Syst.* 6:109-120
- Pond S, Bryan K. 1976. Numerical models of the ocean circulation. *Rev. Geophys. Space Phys.* 14:243-63
- Power SB, Moore AM, Post DA, Smith NR, Kleeman R. 1994. Stability of North Atlantic deep water formation in a global ocean general circulation model. *J. Phys. Oceanogr.*

- 24:904–16
- Pratt LJ, ed. 1990. *The Physical Oceanography of Sea Straits*. Dordrecht: Kluwer. 587 pp.
- Rahmstorf S, Willebrand J. 1995. The role of temperature feedback in stabilizing the thermohaline circulation. *J. Phys. Oceanogr.* 25:787–805
- Redi MH. 1982. Oceanic isopycnal mixing by coordinate rotation. *J. Phys. Oceanogr.* 12:1154–58
- Rhines PB. 1977. The dynamics of unsteady currents. In *The Sea VI*, ed. E Goldberg, pp. 189–318. New York: Wiley
- Rhines PB, Holland WR. 1979. A theoretical discussion of eddy-driven mean flows. *Dyn. Atmos. Oceans* 3:289–325
- Rhines PB, MacCready PM. 1989. Boundary control over the large-scale circulation. In *Parameterization of Small-scale Processes*, ed. P Mueller, pp. 75–99. Honolulu: Hawaii Inst. Geophys. Spec. Publ.
- Rhines PB, Schopp R. 1991. The wind-driven circulation: quasigeostrophic simulations and theory for non-uniform winds. *J. Phys. Oceanogr.* 21:1438–69
- Rhines PB, Young WR. 1982. Homogenization of potential vorticity in planetary gyres. *J. Fluid Mech.* 122:342–67
- Roberts MJ, New AL, Wood RA, Marsh R. 1995. An intercomparison of a Bryan-Cox type ocean model and an isopycnal ocean model. Part 1: the subpolar gyre and high-latitude processes. *J. Phys. Oceanogr.* In press
- Robitaille DV, Weaver AJ. 1995. Validation of sub-grid scale mixing schemes using CFCs in a global ocean model. *Geophys. Res. Lett.* Submitted
- Salmon R. 1986. A simplified linear ocean circulation theory. *J. Mar. Res.* 44:695–711
- Salmon R. 1990. The thermocline as an “internal boundary layer.” *J. Mar. Res.* 48:437–69
- Salmon R, Hollerbach R. 1991. Similarity solutions of the thermocline equations. *J. Mar. Res.* 49:249–80
- Salmon R, Holloway G, Hendershott MC. 1976. The equilibrium statistical mechanics of simple quasi-geostrophic models. *J. Fluid Mech.* 75:691–703
- Sarkisyan AS. 1962. On the dynamics of the origin of wind currents in the baroclinic ocean. *Okeanologia* 11:393–409
- Sarkisyan AS, Ivanov VF. 1971. Joint effect of baroclinicity and bottom relief as an important factor in the dynamics of sea currents. *Izv. Akad. Nauk. Atmos. Ocean. Phys.* 7:173–88
- Sarmiento JL. 1983. A simulation of bomb tritium entry into the Atlantic Ocean. *J. Phys. Oceanogr.* 13:1924–39
- Sarmiento JL. 1992. Biogeochemical ocean models. In *Climate System Modeling*, ed. K Trenberth, pp. 519–51. New York/London: Oxford Univ. Press
- Sarmiento JL, Slater RD, Fasham MJR, Ducklow HW, Toggweiler JR, Evans GT. 1993. A seasonal three-dimensional ecosystem model of nitrogen cycling in the North Atlantic euphotic zone. *Global Biogeochem. Cycles* 7:417–50
- Seager R, Kushnir Y, Cane MA. 1995. A note on heat flux boundary conditions for ocean models. *J. Phys. Oceanogr.* In press
- Seidov DG, Marushkevich AD. 1992. Order and chaos in ocean current dynamics: numerical experiments. *Dyn. Atmos. Oceans* 16:405–34
- Semtner AJ, Chervin RM. 1988. A simulation of the global ocean circulation with resolved eddies. *J. Geophys. Res.* 93:15,502–22
- Semtner AJ, Chervin RM. 1992. Ocean general circulation from a global eddy-resolving model. *J. Geophys. Res.* 97:5493–550
- Semtner AJ, Mintz Y. 1977. Numerical simulation of the Gulf Stream and mid-ocean eddies. *J. Phys. Oceanogr.* 7:208–30
- Song Y, Haidvogel D. 1994. A semi-implicit ocean circulation model using a generalized topography-following coordinate system. *J. Comput. Phys.* 115:228–44
- Spall MA. 1995a. Frontogenesis, subduction, and cross-front exchange at upper ocean fronts. *J. Geophys. Res.* 100:2543–57
- Spall MA. 1995b. Dynamics of the Gulf Stream/deep western boundary current crossover. Part I: Entrainment and recirculation. *J. Phys. Oceanogr.* Submitted
- Speer K, Tziperman E, Feliks Y. 1993. Topography and grounding in a simple bottom layer model. *J. Geophys. Res.* 98:8547–58
- Stevens DP, Ivchenko VO. 1995. The zonal momentum balance in a realistic eddy resolving general circulation model of the Southern Ocean. *J. Phys. Oceanogr.* Submitted
- Stevens DP, Killworth PD. 1992. The distribution of kinetic energy in the Southern Ocean: a comparison between observations and an eddy-resolving general circulation model. *Philos. Trans. R. Soc. London Ser. B* 338:251–57
- Stommel HM. 1961. Thermohaline convection with two stable regimes of flow. *Tellus* 13:224–30
- Stommel HM, Arons AB. 1960. On the abyssal circulation of the world ocean. II. An idealized model of the circulation pattern and amplitude in oceanic basins. *Deep-Sea Res.* 6:217–33
- Suginohara N, Aoki S, Fukasawa MN. 1991. Comments on “On the importance of vertical resolution in certain oceanic general circulation models.” *J. Phys. Oceanogr.* 21:1699–701

- Suginohara N, Aoki S. 1991. Buoyancy-driven circulation as horizontal convection on  $\beta$ -plane. *J. Mar. Res.* 49:295–320
- Suginohara N, Fukasawa M. 1988. Set-up of deep circulation in multi-level numerical models. *J. Ocean Soc. Jpn.* 44:315–36
- Takano K. 1975. A numerical simulation of the world ocean circulation: preliminary results. In *Numerical Models of Ocean Circulation*, ed. RO Reid, pp. 121–29. Washington, DC: Natl. Acad. Sci.
- Thompson JD, Schmitz WJ. 1989. A limited-area model of the Gulf Stream: design, initial experiments, and model-data comparison. *J. Phys. Oceanogr.* 19:791–814
- Toggweiler JR, Dixon K, Bryan K. 1989. Simulations of radiocarbon in a coarse-resolution ocean model. 1. Steady state prebomb distributions. 2. Distributions of bomb-produced carbon 14. *J. Geophys. Res.* 96:8217–64
- Toggweiler JR, Samuels B. 1993a. Is the magnitude of the deep outflow from the Atlantic Ocean actually governed by Southern Hemisphere winds? In *The Global Carbon Cycle*, ed. M Heimann, pp. 303–31. Berlin: Springer-Verlag
- Toggweiler JR, Samuels B. 1993b. New radiocarbon constraints on the upwelling of abyssal water in the ocean's surface. In *The Global Carbon Cycle*, ed. M Heimann, pp. 333–66. Berlin: Springer-Verlag
- Toggweiler JR, Samuels B. 1995a. Effect of Drake Passage on the global thermohaline circulation. *Deep-Sea Res.* In press
- Toggweiler JR, Samuels B. 1995b. Effect of sea ice on the salinity of Antarctic bottom waters. *J. Phys. Oceanogr.* In press
- Treguier AM, McWilliams JC. 1990. Topographic influences on wind-driven, stratified flow in a  $\beta$ -plane channel: an idealized model for the Antarctic Circumpolar Current. *J. Phys. Oceanogr.* 20:321–43
- Tziperman E, Bryan K. 1993. Estimating global air-sea fluxes from surface properties and from climatological flux data using an oceanic GCM. *J. Geophys. Res.* 98:22,629–44
- Tziperman E, Toggweiler JR, Feliks Y, Bryan K. 1994. Instability of the thermohaline circulation with respect to mixed boundary conditions: Is it really a problem for realistic models? *J. Phys. Oceanogr.* 24:217–32
- Veronis G. 1973. Large scale ocean circulation. *Adv. Appl. Mech.* 13:1–92
- Veronis G. 1981. Dynamics of large-scale ocean circulation. In *Evolution of Physical Oceanography*, ed. B Warren, C Wunsch, pp. 140–83. Cambridge, MA: MIT Press
- Verron J, LeProvost E. 1991. Response of eddy-resolved general circulation models to asymmetric wind forcing. *Dyn. Atmos. Oceans* 15:505–33
- Weaver AJ, Aura SM, Myers PG. 1994. Interdecadal variability in an idealized model of the North Atlantic. *J. Geophys. Res.* 99:12,423–41
- Weaver AJ, Marotzke J, Cummins PF, Sarachik E. 1993. Stability and variability of the thermohaline circulation. *J. Phys. Oceanogr.* 23:39–60
- Weaver AJ, Sarachik ES. 1991. Evidence for decadal variability in an ocean general circulation model: an advective mechanism. *Atmosphere-Ocean* 29:197–231
- Webb DJ, Killworth PD, Coward AC, Thompson SR. 1991. *The FRAM Atlas of the Southern Ocean*. Swindon UK: Natural Environ. Res. Council. 67 pp.
- Weisse R, Mikolajewicz U, Maier-Reimer E. 1994. Decadal variability of the North Atlantic in an ocean general circulation model. *J. Geophys. Res.* 99:12,411–21
- Williams RG, Spall MA, Marshall JC. 1995. Does Stommel's mixed-layer 'demon' work? *J. Phys. Oceanogr.* In press
- Winton M, Sarachik ES. 1993. Thermohaline oscillations induced by strong steady salinity forcing of ocean general circulation models. *J. Phys. Oceanogr.* 23:1389–410
- Wolff J-O, Olbers D, Maier-Reimer E. 1991. Wind-driven flow over topography in a zonal  $\beta$ -plane channel: A quasigeostrophic model of the Antarctic Circumpolar Current. *J. Phys. Oceanogr.* 21:236–64
- Yavneh I, McWilliams JC. 1995. Robust multi-grid solution of the shallow-water balance equations. *J. Comput. Phys.* 119:1–25
- Yin FL, Fung IY. 1991. On the net diffusivity in ocean general circulation models. *J. Geophys. Res.* 96:10,773–76
- Yin FL, Sarachik ES. 1995. On interdecadal thermohaline oscillations in a sector ocean general circulation model: advective and convective processes. *J. Phys. Oceanogr.* In press
- Young WR. 1987. Baroclinic theories of the wind-driven circulation. In *General Circulation of the Ocean*, ed. HDI Abarbanel, WR Young, pp. 134–201. Berlin: Springer-Verlag
- Zhang S, Greatbatch RJ, Lin CA. 1993. A reexamination of the polar halocline catastrophe and implications for coupled ocean-atmosphere modeling. *J. Phys. Oceanogr.* 23:287–99